KUOPION YLIOPISTON JULKAISUJA C. LUONNONTIETEET JA YMPÄRISTÖTIETEET 234
KUOPIO UNIVERSITY PUBLICATIONS C. NATURAL AND ENVIRONMENTAL SCIENCES 234

LIZA RASSAEI

Assembly and Characterization of Nanomaterials into Thin Film Electroanalysis

Doctoral dissertation

To be presented by permission of the Faculty of Natural and Environmental Sciences
of the University of Kuopio for public examination in Auditorium in MUC,
Mikkeli University Consortium, Mikkeli,
on Thursday 3rd July 2008, at 12 noon

Department of Environmental Sciences
Laboratory of Applied Environmental Chemistry
University of Kuopio

KUOPION YLIOPISTO

KUOPIO 2008

Distributor: Kuopio University Library
P.O. Box 1627
FI-70211 KUOPIO
FINLAND
Tel. +358 17 163 430
Fax +358 17 163 410
http://www.uku.fi/kirjasto/julkaisutoiminta/julkmyyn.html

Series Editors: Professor Pertti Pasanen, Ph.D.
Department of Environmental Science

Professor Jari Kaipio, Ph.D.
Department of Physics

Author's address: University of Kuopio
Department of Environmental Sciences
Laboratory of Applied Environmental Chemistry
Patteristonkatu 1
FI-50101 Mikkeli, FINLAND
Tel. +358 44 551 7468
Fax +358 15 355 6513
E-mail: Liza.Rassaei@uku.fi

Supervisors: Professor Mika Sillanpää, Dr. Tech
University of Kuopio

Dr. Frank Marken, Ph.D.
University of Bath,
Bath, UK

Reviewers: Professor Marcin Opałło, Ph.D.
Warsaw University,
Warsaw, Poland

Professor Roger J. Mortimer, Ph.D.
University of Loughborough,
Loughborough, UK

Opponent: Dr. Damien W. M. Arrigan, Ph.D.
Tyndall National Institute,
University College, Cork, Ireland

ISBN 978-951-27-0972-4
ISBN 978-951-27-1087-4 (PDF)
ISSN 1235-0486

Kopijyvä
Kuopio 2008
Finland

Rassaei, Liza. Assembly and Characterization of Nanomaterials into Thin Film Electroanalysis. Kuopio University Publications C. Natural and Environmental Sciences 234.2008
ISBN 978-951-27-0972-4
ISBN 978-951-27-1087-4 (PDF)
ISSN 1235-0486

ABSTRACT

New thin film electrodes based on conductive nanoparticles and nanofibers, or nanoporous materials were prepared with potential applications in electroanalysis. For these film preparations, layer by layer assembly, thermal compression, electro-aggregation, and solvent evaporation techniques were used. The prepared films were characterized by electron microscopic methods such as AFM and SEM. Electrochemical behavior of these films was investigated by cyclic voltammetry and impedance electrochemical spectroscopy studies.

In this research, first a novel procedure was suggested for compacting carbon nanofiber (CNF) materials with a polystyrene (PS) binder and additives into highly conducting and repolishable CNF-PS composite electrode. For this new electrode, the capacitive current responses were lowered compared to glassy carbon electrode. Anodic stripping voltammetry experiments for Pb^{2+} system showed the possible application of this electrode in electroanalysis.

In the next work, thin chitosan-carbon nanoparticle films were assembled onto both indium tin oxide and glassy carbon electrode substrates. Amine-ammonium functionalities in chitosan were employed for the immobilization of redox systems (i) via physisorption of indigo carmine and (ii) via chemisorption of 2-methylene-anthraquinone. It was possible to control the number of binding sites within the chitosan-carbon nanoparticle film by changing the thickness of the film deposit or the chitosan content. Voltammetric characteristics and stability of the chemisorbed and physisorbed redox systems were reported as a function of pH.

Then, the highly reactive mesoporous gold film deposits were prepared on a boron doped diamond electrode surface by an electro-aggregation process from 5 nm gold particle colloidal solution. The reactivity of the electro-aggregated gold deposit towards arsenite was investigated in nitric acid and neutral phosphate buffer media. Then, the effect of time, deposition potential, and arsenite concentration were investigated and the lowest detection limit in each system was calculated.

Finally, a porous silicate film from octa anionic cage-like poly silicate and Ru^{3+} cation in an ethanol-based layer by layer process was prepared on ITO/glass electrode. Electrochemical experiments confirmed the formation of redox active ruthenium centers in the form of hydrous ruthenium oxide throughout the film deposit. Three aqueous redox systems were studied in contact with this film. The reduction of cationic methylene blue adsorbed onto the negative surface of the nanocomposite silicate was shown to occur and the polysilicate-Ru^{3+} catalyzed oxidations of hydroquinone and arsenite (III) were investigated. A good electrocatalytic activity of this electrode towards arsenite (III) oxidation showed the potential application of this electrode for arsenite measurements.

Universal Decimal Classification: 543.55, 543.552, 544.6.076.328.3, 620.3

CAB Thesaurus: chemical analysis; analytical methods; electrometric methods; electrochemistry; sensors; electrodes; film; coatings; particles; carbon; chitosan; gold; silicates; ruthenium; voltammetry; impedance; redox reactions; sorption; electron microscopy; arsenite

ACKNOWLEDGEMENT

This study was carried out at the Laboratory of Applied Environmental Chemistry, University of Kuopio, Finland during 2006-2008 in collaboration with the Department of Chemistry, University of Bath, United Kingdom.

Since I was a child, I have had this passion to work in scientific fields in an active research group. There are many people in this way helped me to achieve first stages of this goal. First of all, I am highly grateful to my first supervisor, Prof. Mika Sillanpää, for believing in me, the chance he gave me to study PhD. and pursue my dreams, his encouragements, and his constant support especially for my visits to England. Mika, I know you as a person who has changed my whole life by giving this chance to me. Thanks a lot for making my dreams to come true!

My second supervisor, Dr. Frank Marken, deserves my deepest thanks for inviting me to his lab, giving me the chance to learn from him in science and many other aspects of life, his unconditional support, and his never ending patience. Frank, you inspired me how to be observant and how to grasp any phenomenon with a simple scientific view. You also showed me how to deal with conflicts and difficulties in life. I am also thankful for the extra efforts you put to develop my communication skills ranging from writing to presentation. I am so lucky to have spent part of my graduate studies under the guidance of an intelligent, open minded, forgiving, and beloved person like you. You are indeed my best teacher ever! Many thanks, Frank!

I would like to thank Dr. Mandana Amiri and Dr. Marjana Nousiainen for their comments about thesis material arrangement which saved me a lot of time.

I express my gratitude to my thesis reviewers, Professor Marcin Opałło and Professor Roger J. Mortimer for their fast replies and their valuable comments. I also thank Professor Pertti Pasanen for his great help with edition and publication of my thesis.

I would like to express my sincere thanks to all my friends in laboratory of applied environmental chemistry for their helps and support specially Heikki Särkkä whose help has been countless during my stay in Finland. Thanks Heikki! I also would like to thank our secretary, Berith Zinovjev, whose wise solutions solved my problems many times. Thanks!

Thanks for all the help and company I received from Marken group in Bath especially Michael J. Bonne' who has always been so helpful especially with experimental set ups, and Robert W. French who kindly taught me the lithography on ITO. Thanks Mike and Rob!

I also appreciate Dr. Karen Edler and Hugh Perrott helps with SAXS, SEM, and AFM studies in university of Bath.

I would like to thank all my friends who have been very supportive during my stay in abroad especially Ghazaleh Monjazeb, Sana Owji, Leila Dianati, Pantea Lashgar ara, and Tahmineh Dehdar.

I would like to express my deepest gratitude to my family who has always been supporting me in my studies. To my Parents: Mahdokht Masoud and Dr. Farhang Rassaei, to my sister Janet who has been always ready to help and to my brothers: Farhad, Farzad, and specially Farshad! Thanks for your love and your support!

At the end, I highly acknowledge the financial support from European Union and TEKES which made this opportunity possible to be given to me.

Liza Rassaei

Finland, 2008

ABBREVIATIONS

AFM	Atomic force microscopy
ADH	Alcohol dehydrogenase
AOL	Alcohol oxidase
BDDE	Boron doped diamond electrode
BPPG	Basal plane pyrolytic graphite
CNF	Carbon nanofibers
CNP	Carbon nanoparticles
DDT	Dodecanethiol
DTT	Dothiothreitol
EP	Epinephrine
EDC	1-ethyl-3-(3-dimethylaminopropyl) carbodiimide
GCE	Glassy carbon electrode
GNP	Gold nanoparticles
GOx	Glucose oxidase
Hb	Hemoglobine
HRP	Horseradish peroxidase
ITO	Indium tin oxide
LBL	Layer by layer
MWCNT	Multi wall carbon nanotubes
NHS	N-hydroxysuccinimide
NOPE	2-nitrophenyloctylether
PBS	Phosphate buffer solution
PDDAC	Poly (diallyldimethylammonium chloride)
PS	Polystyrene
PSS	Polysilsesquioxanes
SAM	Self assembled monolayer
SCE	Saturated Calomel electrode
SEM	Scanning electron microscopy
SPM	Scanning probe microscopy
STM	Scanning tunneling microscopy
SWCNT	Single wall carbon nanotubes
TEM	Transmission electron microscopy
WHO	World Health Organization

LIST OF ORIGINAL PUBLICATIONS

This thesis includes a summary of PhD study and five papers which are presented by Roman numbers (**I**-**V**) in the text:

I. L. Rassaei, M. Sillanpää, M. Bonné, F. Marken, Carbon Nanofiber-Polystyrene Composite Electrodes for Electroanalytical Processes, Electroanalysis, 19 (2007), 1461 – 1466.

II. L. Rassaei, M. Bonné, M. Sillanpää, F. Marken, Binding Site Control in a Layer-by-Layer Deposited Chitosan-Carbon Nanoparticle Film Electrode, New Journal of Chemistry, (2008), DOI: 10.1039/b800331a.

III. L. Rassaei, M. Sillanpää, F. Marken. Carbon Nanoparticle - Chitosan Thin Film Electrodes: Physisorption Versus Chemisorption, Electrochimica Acta, Volume 53 (2008), 5732-5738.

IV. L. Rassaei, M. Sillanpää, R. W. French, Richard G. Compton, and F. Marken. Arsenite Determination in the Presence of Phosphate at Electro-Aggregated Gold Nanoparticle Deposits. Electroanalysis, (2008), DOI: 10.1002/elan.200804226.

V. L. Rassaei, M. Sillanpää, E.V. Milsom, X. Zhang, F. Marken, Layer-by-Layer Assembly of Ru^{3+} and $Si_8O_{20}^{8-}$ into Electrochemically Active Silicate Films, J. Solid State Electrochemistry, 12 (2008), 747-755.

CONTENT

1. Introduction

1.1 Nanomaterials

Nanotechnology, the creation of functional materials, devices, and systems through control of matter at the 1-100 nm scale, has become one of the most interesting disciplines in science and technology. The intense interest in nanotechnology is driven by various fields and is leading to a new industrial revolution. A scientific and technical revolution has just begun based upon the ability to systematically organize and manipulate matter at nanoscale. This highly multidisciplinary field is strongly related to fundamental sciences such as physics, chemistry, and biology (Merkoçi 2007). Nanotechnology has brought new possibilities for sensor constructions and for developing novel electrochemical assays.

Nanoscale materials have been used to achieve direct writing of enzymes to electrode surface, to promote electrochemical reactions, and to amplify signal of recognition events (Pumera et al. 2007). The unique properties of these materials offer excellent prospects for interfacing analytical recognition events with electronic signal transduction and for designing a new generation of electronic devices exhibiting new functions (Wang 2005). In this regard, nanomaterials are attractive building blocks in nanotechnology because of their extremely small size feature, large surface to volume ratio, high packing densities, unusual target binding properties, and overall structural robustness (Rosi et al. 2005).

The size of nanomaterials can be an advantage over a bulk structure, simply because a target binding affects on its physical and chemical properties which can not be seen in bulk structure of the same materials (Heath 1995). These materials are tailorable which is an important aspect in new nanodevice designing. New synthesis, fabrication, and characterization methods for nanomaterials have evolved to the point that deliberate modulation of their size, shape, and composition is possible allowing accurate control of their properties. Nanomaterials are very well suited for chemical sensor applications, because their physical properties often vary considerably in response to changes of the chemical environment.

1.2 Forms of nanomaterials

Nanomaterials constitute an emerging subdiscipline in the chemical and materials sciences (Ozin 1992). All conventional materials like metals, semiconductors, glass, ceramic or polymers can in principle be obtained with a nanoscale dimension. Nanomaterials have various microstructural features such as nanoparticles (including quantum dots), nanowires, nanotubes, nanocoatings, and nanocomposites. Here, the most common nanomaterials and their well known characteristics are introduced.

1.2.1 Fullerenes

Fullerene, C_{60}, was discovered in 1985 (Kroto et al. 1985) using the laser evaporation of graphite. It is considered to be the 3rd form of carbon in addition to diamond and graphite. Unlike graphite or diamond, fullerenes are closed-cage carbon molecules consisting of a number of five-membered rings and six-membered rings including 60, 70, or more carbon atoms. They consist of a spherical, ellipsoid, or cylindrical arrangement of dozens of carbon atoms. Spherical fullerenes are often called "buckyballs", whereas cylindrical fullerenes are known as "buckytubes", or "nanotubes". Fullerene derivatives show a plethora of interesting properties, ranging from superconductivity to ferromagnetism and promise future applications in batteries, transistors, and sensors (Margadonna et al. 2002). Fullerene C_{60} with 60 π-electrons potentially can be expected to be applied as a good adsorbent to adsorb and detect nonpolar, and some polar organic molecules. However, fullerene cannot adsorb metal ions, anions and most polar organic species. Because of their unique structures and properties, fullerenes have obtained a lot of attentions from physicists, chemists, biologists, and engineers. These materials have been used for designing chemical sensors (Shih et al. 2001 & Lin et al. 2003), as gas adsorbent (Hayashi et al. 2004), in medical science for HIV inhibition (Marchesan et al. 2005), DNA photocleavage (Miyata et al. 1999), and in electrosensors (Shiraishi et al. 2007).

1.2.2 Nanotubes

Nanotubes offer significant advantages over most existing materials such as carbon fiber. Carbon nanotubes are of fullerene-related structures that consist of graphite cylinders closed at either end with caps containing pentagonal rings. This group includes nanotubes, nanowires, nanobelts, and nanorods.

Multi wall carbon nanotubes (MWCNT) have become known since 1991 (Iijima 1991) through vaporizing carbon graphite with an electric arc under an inert atmosphere and its chemical vapor deposition. Depending on the synthesis conditions, either single or multiwall carbon nanotubes are formed. Single wall nanotubes are single cylinders of graphite sheet and multiwall nanotubes are multi concentric cylinders of graphite sheets.

The basic constitution of the nanotube lattice is the C-C covalent bond as in graphite planes which are one of the strongest in nature (Ajayn 1999). The strength of the sp^2 carbon-carbon bonds gives carbon nanotubes amazing mechanical properties (Treacy et al. 1996). The tensile strength or breaking strain of nanotubes is around 50 times higher than steel. The electronic properties of carbon nanotubes are also extraordinary. Especially notable is the fact that nanotubes can be metallic or semiconducting depending on their structure. Thus, some nanotubes have conductivities higher than that of copper, while others behave more like silicon. There is a great interest in the possibility of constructing nanoscale electronic devices from nanotubes (Ren et al. 1998), and some progress is being made in this area (Collins et al. 1997). There are several areas of technology where carbon nanotubes are already being used. These include flat-panel displays (Zhang et al. 2001), scanning probe microscopes (Dai et al. 1996), and sensing devices (Fukuda et al. 2004). The unique properties of carbon nanotubes will undoubtedly lead to many more applications in future.

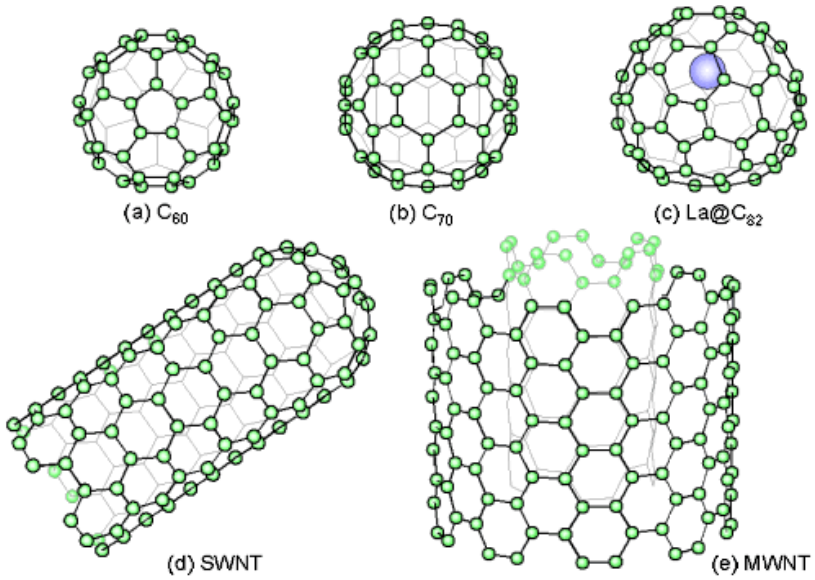

Figure 1. Closed caged molecules of carbon (a) C_{60} (b) C_{70} (c) an endohedral metal fulleride, (d) a single wall carbon nanotube, and (e) a multi wall carbon nanotube (with kind permission from Shigeo Maruyama)

1.2.3 Carbon nanofibers

Carbon nanofibers (CNF) are produced from the catalytic decomposition of hydrocarbon gases or carbon monoxide over selected metal particles that include iron, cobalt, nickel, and some of their alloys at high temperatures. They are hollow cylinders with diameters around one hundred nanometers and lengths of a few tens of microns arranged as stacked cones, cups, or plates (Arvinte et al. 2007). The mechanical strength and electronic properties of CNFs are similar to CNTs. The advantages of carbon nanofibers over carbon nanotubes are due to a dramatic cost difference and the fact that carbon nanofibers have graphene edge planes, which are ledges of carbon that protrude from the surface of the nanofibers at regular intervals leading to easier physical bonding with other materials; a property that is useful when creating integrated composites of polymers and carbon fibers. They have a 2 to 100 times larger diameter compared to MWCNT or SWCNT and are less crystalline (with a kind of cup-stacked or stacked coin structure) (Price et al. 2003). Carbon nanofiber materials are of interest for applications such as high surface area electrode materials, e.g. for energy storage (Steigerwalt et al. 2002), in electroanalysis (Musameh et al. 2002), or as support for catalysts (Vieira et al. 2003).

1.2.4 Nanoparticles

Nanoparticles are of great scientific interest as they effectively make a bridge between bulk materials and atomic or molecular structures. Nanoparticles are solid particles with diameters in the

range of 1-100 nm. These particles can be single crystallites, aggregates of crystallites, or non-crystalline, and with different morphologies such as spheres, cubes, and platelets (Cao 2004). Nanoparticles are larger than individual atoms but smaller than bulk solids. The properties of these materials change as their size approaches the nanoscale and as the percentage of atoms at the surface of a material becomes significant. These materials can be prepared from a variety of materials such as carbon, metals, semiconductors, oxides, proteins, or synthetic polymers through different approaches. Methods to produce nanoparticles from atoms are chemical processes based on transformations in solution e.g. sol-gel processing, chemical vapour deposition (CVD), plasma or flame spraying synthesis, laser pyrolysis, and atomic or molecular condensation. These chemical processes rely on the availability of appropriate "metal-organic" molecules as precursors.

The small size is not the only requirement to form nanoparticles. There are some characteristics that are needed for the nanoparticles to be useful for any practical applications including:

1. Uniform size distribution
2. Identical shape, chemical composition, and crystal structure within individual particles and among different particles.
3. Dispersion

Nanoparticles can bring four unique advantages when used in electroanalysis: enhancement of mass transport, catalysis, high effective surface area, and control over electrode microenvironment (Welch et al. 2006). They can be used in a variety of analytical and bioanalytical formats for electrochemical detection. When nanoparticles are used as quantitation tags, an electrical/electrochemical signal emanating from the particles is quantified. Encoded nanoparticles used as labels rely on one or more identifiable characteristics to allow them to serve as encoded electrochemical hosts for multiplexed bioassays. This is analogous to the positional encoding of assays on microarrays, but in solution (Penn et al. 2003).

1.2.5 Nanocomposites

Nanocomposites refer to materials consisting of at least two phases with one dispersed in another and one or more of the phases have at least one dimension of order 100 nm or less. An important microstructural feature of a nanocomposite is the large ratio of interphase surface area to volume. The entire matrix is almost located at the interface of the nanofiller and thus the nanocomposite properties are dominated by interfacial interactions. Therefore, nanocomposites display properties that are superior to those of either of the pure component phases and even to those of the conventional composites (Kojima et al. 1993).

The ability to create composites with well-controlled structures on the nanometer scale, nanocomposites, is of great interest for diversified applications. The nanostructures with large specific surface area could provide an important and feasible platform for catalysis (Shokouhimehr et al. 2007), sensing (Pimtong-Ngam et al. 2006), separation (Zhou et al. 2007), sorption (Bobet et al. 2007), and fuel cells (Song et al. 2004). The use of nanoparticles and nanostructures producing mass transport/electron transfer channels would enhance remarkably both electron transfer and mass transportation, particularly in the unusual charge / mass transport mechanisms in a

nanostructured network with electrocatalytic properties (Crespilho et al. 2006). There are a large number of methods for synthesis and fabrication of nanostructured composites demonstrated in literature. Among them, a simple and effective way is to introduce nanoparticles/nanotubes into polymer matrices, or simply to mix them with the polymer matrices (Dalmas et al. 2005, Singha et al. 2006).

1.2.6 Microporous and Mesoporous Materials

Microporous and mesoporous materials are porous solids with defined pore size in nanometer range (Kresge et al. 1992). Depending on the pore size, porous solids can be classified into three groups:

1. Microporous materials with pore sizes <2 nm
2. Mesoporous materials with pore sizes of 2 nm-50 nm
3. Macroporous materials with pore sizes> 50 nm

Ordered micro and mesoporous materials are high performance materials for catalysis or highly selective adsorbents, but in addition they provide excellent opportunities for the creation of materials with additional functionality. Their regular pore system can be used to introduce molecules or particles that are stabilized by the solid framework. Zeolites are the most important microporous materials which are commercially available (Schüth et al. 2002).

1.3 Important tools to characterize nanomaterials

The ability to characterize materials at the nanoscale is the key to the development of nanotechnology in general. The rapid advances in nanotechnology are linked to the discovery and to the improvement of the instruments used to measure and manipulate individual structure with atomic resolution with extreme sensitivity and accuracy. This allows researchers to discover and study new chemical, physical, and biological phenomena and applications for nanomaterials.

Scanning probe microscopes and high resolution electron microscopes have a crucial role in nanomaterials characterization as they provide the most direct information of individual nanomaterials and their structural properties (Cao 2004) whereas bulk methods could be used to characterize the collective features of nanomaterials. The important tools to characterize nanomaterials are introduced below.

1.3.1 Electron microscopy

Electron microscopy is an imaging technique which uses a beam of highly energetic electrons to examine objects on a very fine scale. Topography, morphology, composition, and crystallographic structure are among information which can be obtained by this probe (Sherrington et al. 1988). In this technique, a stream of electrons is formed and accelerated toward the sample using a high electrical field, 10-100 KeV. This stream is confined using metal apertures into a thin beam which then focused in to a typical spot with diameter of 1-100 nm on the sample using magnetic field

lenses. The use of electron beams requires the sample be placed in a vacuum chamber for the analyses. When the electron beam strikes the sample, various interactions can occur. These interactions are detected and transformed to characteristic information of the sample.

Scanning electron microscope (SEM) and transmission electron microscope (TEM) are two common types of electron microscopes explained in more details in the next section.

1.3.1.1 Scanning electron microscopy

SEM is a method for high-resolution imaging of surfaces. The SEM uses electrons for imaging, like a light microscope which uses visible light. A finely focused electron beam scanned across the surface of the sample generates secondary electrons, backscattered electrons, and characteristic X-rays. These signals are collected by detectors to form images of the sample displayed on a cathode array tube screen. SEM typically is used for conductive samples. Scanning electron microscopy is one of the most widely used techniques in nanomaterials characterization. This method usually is applied to get information about the grain size, surface roughness, porosity, particle size distributions, material homogeneity, and intermetallic distribution and diffusion (Bowman et al. 1997).

1.3.1.2 Transmission electron microscopy

TEM is a microscopy technique whereby a beam of electrons is transmitted through an ultra thin specimen, interacting with the specimen as it passes through it. The energy of electrons in TEM determines the lateral spatial resolution and the relative degree of penetration of electrons in specific samples. In addition to the capability of structural characterization, TEM has been explored for a wide range of applications in nanomaterials (Cao 2004). This includes the determination of the crystal structure and lattice parameter of individual nanomaterials and the measurement of mechanical properties of individual nanotubes and nanowires (Wang 2000).

1.3.2 Scanning probe microscopy

SPM is a general term for a family of microscopes (Binnig et al. 1982). It is a recent characterization technique which enables to probe a surface at nanometer scale. In this technique, a sharp probe tip is scanned over a surface and it measures local physical and chemical properties of the surface. As in this method, no beam of light or electron is used; resolution is not limited by wavelength of light or electrons. The probe size and movement accuracy over the surface limit the resolution. In this technique, the surface is imagined at atomic resolution and it is possible to get 3-D maps of the surface. Depending on the interaction type of tip and sample surface, various types of SPM have been developed. SPM provides information beyond topography and can be used to examine many local properties such as electronic structure, optical properties and magnetism (Andersen et al. 1999).

Scanning tunneling microscopy (STM) and atomic force microscopy (AFM) are two important techniques of scanning probe microscopy.

1.3.2.1 Scanning tunneling microscopy

STM works by scanning a very sharp metal wire tip over a surface. By bringing the tip very close to the surface, and by applying an electrical voltage to the tip or sample, it is possible to image the surface at an extremely small scale-down to resolving individual atoms. The operation of a scanning tunneling microscope (STM) is based on the so-called tunneling current, which starts to flow when a sharp tip approaches a conducting surface at a distance of approximately one nanometer. The tip is mounted on a piezoelectric tube, which allows tiny movements by applying a voltage at its electrodes. Thereby, the electronics of the STM system control the tip position in such a way that the tunneling current and, hence, the tip-surface distance is kept constant, while at the same time scanning a small area of the sample surface. This movement is recorded and can be displayed as an image of the surface topography (Vansteenkiste et al. 1998).

1.3.2.2 Atomic force microscopy

AFM is one of the most powerful tools for determining the surface topography of native biomolecules at subnanometer resolution. The technique involves imaging a sample through the use of a probe, or tip, with a radius of 20 nm. The tip is held several nanometers above the surface using a feedback mechanism that measures surface–tip interactions on the scale of nanoNewtons. Variations in tip height are recorded while the tip is scanned repeatedly across the sample, producing a topographic image of the surface (Claesson et al. 1996). Atomic force microscope is capable to produce images in different modes including tapping, magnetic force, electrical force, and pulsed force.

1.4 Electrochemistry and electroanalysis

Electrochemistry is the branch of chemistry concerned with the interrelation of electrical and chemical effects. A large part of this field is the study of reactions in which charged particles (ions or electrons) cross the interface between two phases of matter, typically a metallic phase (the electrode) and a conductive solution, or electrolyte. A process of this kind can always be represented as a chemical reaction and is known generally as an electrode process. Electrode processes (also called electrode reactions) take place within the double layer and produce a slight unbalance in the electric charges of the electrode and the solution. Much of the importance of electrochemistry lies in the ways that these potential differences can be related to the thermodynamics and kinetics of electrode reactions. In particular, manipulation of the interfacial potential difference affords an important way of exerting external control on an electrode reaction (Bard 2001).

Electrochemistry affords some of the most sensitive and informative analytical techniques. Electroanalytical chemistry plays a very important role in the protection of our environment. In particular, electrochemical sensors and detectors are very attractive for on-site monitoring of priority pollutants, as well as for addressing other environmental needs. Such devices satisfy many of requirements for on-site environmental needs. They are sensitive and selective towards electroactive species, fast and accurate, compact, portable, and in expensive (Ashley 2003).

Several electrochemical devices, such as pH or oxygen electrodes, have been used for years in environmental analysis. Recent advances in nanotechnology and electrochemical sensor technology will certainly expand the scope of these devices towards a wide range of organic and inorganic contaminants and will facilitate their role in field analysis. In recent years, the progress in ultramicroelectrodes, development of ultra trace voltammetric techniques, design of new tailored interfaces and the microfabrication of molecular devices have led to substantial increase in the popularity of electroanalysis. Indeed, electrochemical probes are receiving a major share of the attention in the development of chemical sensors (Wang 2000).

Electroanalysis is the interplay between electricity and chemistry in which a quantity of electricity such as current, potential, or charge is measured and it is related to chemical parameters. An electrochemical sensor should provide reliable information about the change in chemical composition of its environment. Ideally, such devices are capable of responding continuously and reversibly. In electrochemical sensors, the analytical information is obtained from the electrical signal that results from the interaction of the target analyte and the recognition layer. Different electrochemical devices can be used for the task of environmental monitoring depending on the nature of the analyte, the character of the sample matrix, and sensitivity, or selectivity requirements (Brett 1999).

Electroanalytical methods such as cyclic voltammetry, stripping voltammetry, differential pulse voltammetry, and chronoamperometry are not only capable of assaying trace concentrations of an electroactive analyte, but supply useful information concerning its physical and chemical properties. Quantities such as oxidation potentials, diffusion coefficients, electron transfer rates, and electron transfer numbers are readily obtained using electroanalytical methods, and difficult to obtain using other techniques. Electroanalytical methods can also be combined with spectroscopic techniques in situ to provide information concerning molecular structures and reaction mechanisms of transient electroactive species (Scholz et al. 2002). The most popular electroanalytical technique is cyclic voltammetry.

1.5 Cyclic voltammetry

Cyclic voltammetry or CV is one of the most effective and versatile electroanalytical tools and it has become very popular for initial electrochemical studies of new systems (Bard 2001). The power of cyclic voltammetry results from its ability to rapidly provide considerable information on the thermodynamics of redox processes, on the kinetics of heterogeneous electron-transfer reactions, and on coupled chemical reactions or adsorption processes. Cyclic voltammetry is often the first experiment performed in an analytical study as it offers a rapid location of redox potentials of the electroactive species (Wang 2000).

In this technique, the input potential signal is a triangular function and the potential of a stationary working electrode is scanned linearly by means of potentiostat and the resulting current is monitored. When the current is plotted versus the potential, a cyclic voltammogram curve is obtained. There are two different regions can be recognized in the resulting cyclic voltammogram; anodic (positive current values) and cathodic (negative current values) where the oxidation and reduction reactions take place, respectively. The peak current on this voltammogram shows the

potential where the electrode reactions take place. The potential, shape, and the height of the peak current are functions of scan rate, electrode materials, and solution composition.

The cyclic voltammetry is characterized by several important parameters. Four of these are two peak currents and two peak potentials. The peak size and peak potential seen on the forward and backward scan reflects the reversibility of reaction (Fisher 1996). Generally, two limiting cases of studied systems do exist. It is a reversible electrode process and an irreversible electrode process.

1.5.1 Reversible electrode reactions

When the ratio of C_{Ox}/C_{Red} near the electrode surface follows Nernst equation, the kinetics of the process is controlled by reactant diffusion. This is the case for a reversible redox couple and the peak current, i_p, is described by the Randles-Sevcik equation (Randles 1948):

$$I_P = (2.69 \times 10^5) n^{\frac{3}{2}} A C D^{\frac{1}{2}} v^{\frac{1}{2}} \qquad (1)$$

where n is the number of moles of electrons transferred in the reaction, A is the area of the electrode, C is the analyte concentration (in moles/cm^3), D is the diffusion coefficient, and v is the scan rate of the applied potential.

The ratio of the reverse to forward peak currents, $I_{p,r}$ /$I_{p,f}$ is unity for a simple reversible couple.

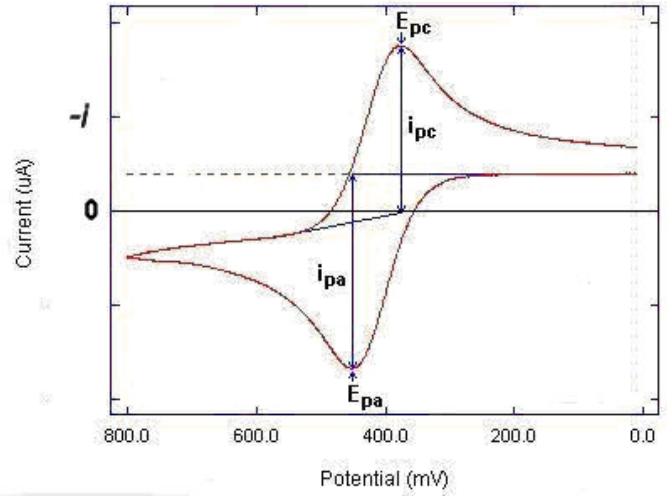

Figure 2. A typical cyclic voltammetry (adapted from Fisher 1996)

The potential of the peaks on the potential axis (E_p) is related to the formal potential of the redox process. The formal potential for a reversible couple is centered between $E_{p,a}$ and $E_{p,c}$:

$$E^0 = \frac{E_{p,a} + E_{p,c}}{2} \qquad (2)$$

Here, the peak potential difference is temperature dependent and at 298 K, the peak separation between peak potentials is 59 mV/n. Therefore, the peak separation can be used to determine the number of electrons transferred. Both anodic and cathodic potentials are independent of scan rate in this case (Bard et al. 2001).

1.5.2 Irreversible electrode reactions

For irreversible processes, the boundary condition on the surface of electrode is given by kinetics of electrode reaction instead of Nernst equilibrium. In this case, the peak current is given by:

$$I_p = (2.99 \times 10^5) n(\alpha n_a)^{\frac{1}{2}} ACD^{\frac{1}{2}} v^{\frac{1}{2}} \qquad (3)$$

where α is the transfer coefficient. The peak current is lower in height than reversible systems and depends on the value of α.

In this case, the individual peaks are reduced in size and widely separated. Totally irreversible systems are characterized by a shift in peak potential with change in scan rate:

$$E_p = E^0 - \frac{RT}{\alpha n_a F}\left[0.78 - \ln\frac{k^0}{D^{\frac{1}{2}}} + \ln\left(\frac{\alpha n_a F v}{RT}\right)^{\frac{1}{2}}\right] \qquad (4)$$

Where n_a is the number of electrons involved in the charge transfer step and k^o is the rate constant. Therefore, E_p occurs at potentials higher than E^o, with over potentials related to α and k^o (Wang 2000).

1.6 Nanomaterials in electroanalysis

Electroanalysis is one of the best methods for detecting species in solution due to its low cost, ease of use, and reliability (Welch et al. 2006). Most developments in electroanalytical chemistry in recent years have originated from advances in sensor design, chemical modification, and functionalization of electrodes for enhanced sensitivity and selectivity of electroanalysis. Nanomaterials have added a new dimension to electroanalysis and electrode development. The unique properties of these materials have led to simple, high sensitive electroanalytical procedures that could not be accomplished by standard electrochemical methods. Nanomaterials have brought four main advantages to a modified electrode when compared to a microelectrode; among them are high effective surface area, mass transport, catalysis, and control over local microenvironment

(Katz et al. 2004). A broad range of nanomaterials especially nanotubes and nanoparticles with different properties have found wide applications in many analytical methods (Penn et al. 2003).

1.6.1 Carbon nanofibers

Among many carbon nanomaterials, carbon nanofibers are the subject of extensive experimental and theoretical studies for specific applications. Their use in electrochemical sensors is based on the fact that these materials can play dual roles. They can be used as immobilization matrix for special molecules and at the same time they are used as a transducer to produce the electrochemical signal (Arvinte et al. 2007).

In 2001, carbon nanofibers with diameters in the range of 10–500 nm were introduced as novel electrode materials for electrochemical applications for the first time (Marken et al. 2001). In this study, both porous and nonporous electrode configurations were prepared separately. For porous electrode configuration, carbon nanofibers were held in place against a 3 mm diameter glassy carbon electrode by a Lycra™ membrane having a 0.2 mm pore size and for nonporous one, carbon nanofibers were embedded in a high-melting paraffin wax packed in a Teflon tube and then degassed under vacuum. It was shown that the high surface area combined with facile solution penetration into the space between the fibers allows a high capacitance to be achieved for the porous electrode configuration. In contrast to these materials, low capacitance currents and high faradaic currents are achieved by embedding the fibers in a high-melting paraffin wax in the nonporous electrode configuration. The nonporous electrode successfully was applied in the cathodic deposition and anodic stripping of Pb metal. This study showed that carbon nanofiber materials have potential use in electroanalytical applications.

At the same year, the method to prepare a new nanoporous carbon nanofiber nanocomposite electrode with black wax was developed (Dijk et al. 2001). In brief, carbon nanofiber were placed in a sealed Teflon tube and evacuated. Then, black wax was melted by heating under the vacuum and forced into the tube under pressure. The experiments for reduction of 1 mM $Ru(NH_3)_6^{3+}$ in 0.1 M KCl showed an almost sigmoidal and not classical dependence of peak height on $(\text{scan rate})^{1/2}$. From which, it implied that the electrode surface behaved more like an assembly of microelectrodes than a planar electrode. This electrode then was successfully applied for detection of zinc in 1.0 M HCl and the best signal to noise ratio was achieved for the scan rate of 40 Vs^{-1}. Then, the interference effect of Pb^{2+} on the stripping peak of Zn was investigated. So, the resulting nanocomposite electrodes showed good conductivity, a wide potential window in aqueous solutions, low background currents; near steady state voltammetric responses with substantial Faradaic currents and sharply peaked fast scan metal stripping responses. These advantages make them a good candidate for new generation of electrode materials.

In 2003, a new carbon nanofiber electrode was grown into a porous ceramic substrate in the presence of nanoparticulate Fe_2O_3 as a catalyst precursor, (Murphy et al. 2003). This carbon nanofiber–ceramic fiber composite electrode was proved to be electrically conductive and mechanically robust. The use of this electrode for adsorption of aromatic compounds such as hydroquinone, benzoquinone, and phenol showed its potential application in electroanalysis.

In 2005, the carbon nanofiber composite electrode was prepared for use in liquid|liquid redox systems (Shul et al. 2005). In this study, two different electrodes were prepared and compared. First electrode was prepared with carbon nanofiber added to a hydrophobic sol-gel matrix. The second electrode was a carbon nanofiber paste electrode. Both electrodes were modified with redox probe solution in 2-nitrophenyloctylether. For both electrodes, enhanced voltammetric currents for the transfer of anions at liquid|liquid phase boundaries presumably by extending the triple-phase boundary was obtained. Both anion insertion and cation expulsion processes were observed driven by the electro-oxidation of decamethylferrocene within the organic phase. A higher current response was obtained for the more hydrophobic anions such as ClO_4^- or PF_6^- when compared to that for more hydrophilic anions like F^- and SO_4^{2-}.

In 2006, a novel hydrophobic carbon nanofibers–silica composite modified electrode has been prepared using a sol–gel methodology on ITO/glass substrate (Niedziolka et al. 2006). The hydrophobic film electrode was then modified with two types of redox liquids: pure *tert*-butylferrocene or dissolved in 2-nitrophenyloctylether (NOPE) as a water-insoluble solvent. Both electrodes then were immersed in aqueous electrolyte solution. It was demonstrated that the electrode seems to have gas entrapped in the hydrophobic mesoporous structure when immersed in purely aqueous solution causing partial blocking of the electrode. Conversely, well-defined voltammetric responses were observed when the electrodes were wetted with organic redox liquids such as *t*-BuFc or its solutions in NPOE; the effect of the CNFs on the voltammetric signal was also shown. The presence of CNF composite film was shown to have a big effect on the efficiency of electrode process of redox liquid deposit and its stability in voltammetric conditions. The anion selectivity is also exposed for the electrode modified with supported NPOE film. In this case, it is possible to extract ions from aqueous phase for example in flow systems or other electroanalytical techniques.

Carbon nanofiber was mixed with silicon oil in order to create a paste electrode (Pruneanu et al. 2006). The cyclic voltammetry of this type of electrode in ferrocenecarboxylic acid solution showed the redox process is quasi-reversible, and it involves the transfer of electrons between Fe (II) and Fe (III). Then, the same mediator was used to make a second-generation glucose biosensor. The mediator was co-immobilized with the enzyme in the carbon nanofibers paste. The sensor linearly responded to glucose. Also, the oxidation of calf thymus DNA at the carbon nanofiber paste electrode was investigated by differential pulse voltammetry. A clear signal, due to guanine oxidation, was obtained in the case of single-stranded DNA. This study was a new proof for use of carbon nanofiber materials in biosensor devices.

At the same year, a thin film of carbon nanofibers embedded into a hydrophobic sol-gel material onto ITO/glass electrode substrate was suggested for ion transfer process at liquid|liquid solution interface (Rozniecka et al. 2006). It was shown that the redox processes within the ionic liquid could be coupled to ion transfer processes at the ionic liquid|water. In this study, carbon nanofibers material provided an ideal porous support and enhanced both capacitive background and faradaic current response. Ion transfer processes accompanying the capacitive current charging of the high surface area CNF electrode was proposed. Conjunction of simple redox systems with a high surface area CNF electrode for stable ion transfer voltammograms in ionic liquid|aqueous electrolyte systems was suggested for future applications in selective and specific ion transfer electrodes.

In another study, a highly activated carbon nanofiber electrode was also prepared for the design of catalytic electrochemical biosensor of glucose (Vamvakaki et al. 2006) with direct immobilization of enzymes onto the surface of carbon nanofiber. The very high surface areas of nanofibers, together with their large number of active sites, provided the base for the adsorption of enzymes and proteins. Furthermore, both direct electron transfer and more stability of the enzymatic activity were allowed in this work. In this study, it was proved that carbon nanofiber materials are the best matrix for immobilization of proteins and enzymes in compare with carbon nanotubes and graphite. These materials were suggested as very promising substrates for the development of highly stable and novel biosensors.

In contrast to previous works which had used the random arrays of carbon nanofibers in electrode design, a vertically aligned carbon nanofiber electrode was developed for immobilization of the metalloprotein cytochrome *c* (Baker et al. 2006). In this work, the immobilization of cytochrome *c* was successfully occurred on carboxylic acid groups resulted from photochemical functionalization of carbon nanofibers. Although a higher electrochemical current response due to larger surface area was obtained in this study, the signal to noise ratio was reduced due to high capacitive current. The reason for this was explained as inhomogeneity of carbon nanofiber functionalization at edge plane versus basal plane sites.

It was demonstrated that with a simple one step electrochemical polymerization of thionine, carbon nanofiber nanocomposite and alcohol oxidase (AOL), a stable poly(thionine)-CNF/AOL biocomposite film was formed on the glassy carbon electrode surface (Wu et al. 2007). A sensitive ethanol biosensor was obtained based on the excellent catalytic activity of the biocomposite film toward reduction of dissolved oxygen. It was showed that this electrode has excellent characteristics and performance such as low detection limit, fast response and good stability. From this work, it became clear that electrochemical electropolymerization method is also suitable for carbon nanofiber sensor construction.

A carbon nanofiber modified glassy carbon electrode was shown to be able of oxidizing the NADH cofactor at lower potential compared to unmodified GC electrodes (Arvinte et al. 2007). In another work at the same year, an amperometric sensor for NADH and ethanol was prepared with soluble carbon nanofiber materials (Wu et al. 2007). These materials showed good dispersion and wettability. In brief, the prepared carbon nanofiber solution was cast on glassy carbon electrode. In order to modify this electrode as an amperometric biosensor, an aliquot of ADH solution was dropped on pretreated GCE and after dryness, CNF solution was added twice to the membrane. This electrode demonstrated a very efficient electrocatalytic behavior toward the oxidation of NADH at a low over potential due to the formation of high amount of oxygen rich groups. The accelerated electron-transfer kinetics limits the formation of electrode surface fouling and improves the operational stability, fabrication reproducibility, and sensitivity of CNF-based sensors. From comparison of both studies, it can be seen that the second electrode with carboxylic acid functional groups in its structure can decrease the overpotential needed for oxidation of NADH by 273mV more and lower the detection limit 100 times less than the first electrode.

An amperometric glucose sensor was designed based on the catalytic reduction of dissolved oxygen at soluble carbon nanofiber (Wu et al. 2007). In this study, the carbon nanofiber materials were functionalized in acidic media to obtain carboxylic groups. It was proved that these groups improve the CNF solubility and biocompatibility. This electrode showed good conductivity to

accelerate the electron transfer of electroactive compounds and excellent catalytic activity towards reduction of oxygen which can be used for continuous monitoring of dissolved oxygen in different systems.

Another amperometric sensor was developed based on covalent immobilization of an immunoassay with thionine on carbon nanofiber materials (Wu et al. 2007). For this immunosensor preparation, a small aliquot of CNF solution was dropped on the pretreated glassy carbon electrode and dried. Then it was immersed in a solution containing EDC and NHS. After rinsing the activated CNF/GCE, the electrode was immersed in a mixture of carcinoma antigen-125 and thionine in order to modify the electrode. The immobilized HRP-labeled immunoconjugate showed good enzymatic activity for the oxidation of thionine by hydrogen peroxide. From this research, it was cleared that carbon nanofiber can effectively immobilize antigen and it could be used in the preparation of other immunosensors for the detection of important antigens.

A carbon nanofiber doped chitosan film was prepared as a sensitive impedance sensor for cytosensing (Hao et al. 2007). To prepare this nanocomposite electrode, the nitric acid treated carbon nanofiber was dispersed in chitosan solution. The large number of oxygen groups greatly enhances the hydrophilicity of CNF and it can interact with the reactive amino and hydroxyl functional groups in chitosan. Then, by applying potential and change in pH at electrode surface, chitosan hydrogel incorporated with CNF was electrodeposited on the cathode surface. The prepared electrode was then simply modified by casting a small amount of cell solution. This sensor showed good fabrication reproducibility and detection precision. This work showed the new application of CNF in electroanalysis for clinical testing.

From these studies, it can be concluded that CNF is a very promising material based on its nanostructure and properties (Yoon et al. 2004). Oxidation of CNF with nitric acid can produce carboxyl groups without degradation of the structural integrity of its backbone. Compared to carbon nanotubes CNF has a much larger functional surface area and higher ratio of surface active groups to volume. Thus, it can be used for covalent binding of proteins and mediators with the help of a cross-linking reagent. The covalent attachment of proteins to the CNF surface overcomes the problems of instability and inactivation (Wu et al. 2007). Therefore, CNF is a new and promising material for designing next generation of sensors for electroanalytical monitoring in different fields.

1.6.2 Carbon nanoparticles

Carbon nanoparticles or carbon blacks represent very interesting carbon materials which offer all the advantage of nanocarbons such as conductivity, high surface area, and adsorption sites. They are particulate forms of highly dispersed elemental carbon (MacDonald et al. 2008). These materials similar to metal nanoparticles (Welch et al. 2006) are very interesting building blocks in electrode systems and their high level of interfacial edge sites are potentially useful in electrochemical processes (Banks et al. 2005).

In 2003, for the first time carbon nanoparticles were used as electrode materials for a sensor preparation (Zimer et al. 2003). This electrode was prepared by the dispersion of template carbon

nanoparticles onto polyaniline. This new nanocomposite electrode showed excellent chemical and physical stabilities and it was applied as a sensor for detection of Cu^{2+} and Pb^{2+} ions. The association of the polymeric matrix with template carbon nanofiber allowed the quantification of low concentrations of copper and lead showing the electroanalytical application of this composite electrode.

Carbon nanoparticles were used in an electrostatically layer by layer assembly method with poly (diallyldimethylammonium chloride) on ITO/glass electrode surface to make an ultrathin nanocomposite for electroanalytical purposes (Amiri et al. 2007). It was demonstrated that absorption into the CNP-PDDAC composite film is dominated by positive binding sites in the PDDAC. Therefore, the negatively charged molecules such as indigo carmine can strongly bind to this film. It was also shown that the effect of the CNP-PDDAC film deposit on particular redox systems depends on the molecular characteristics as well as the film thickness. This film was successfully applied to distinguish dopamine from ascorbate in mixed redox system with a considerable peak separation of 230 mV. This research showed the possible use of this film in electroanalysis of an important neurotransmitter. In another work, this film was used to determine triclosan as an anti-fungal and anti-bacterial compound with a negatively charged chlorinated poly aromatic phenol in its structure at high pHs (Amiri et al. 2007). Due to its negative charge, triclosan was demonstrated to be accumulated into CNP-PDDAC film simply by electrostatic interaction. In this research, the application of this film in electroanalysis was shown and its possible application in anodic extraction due to positively charged amine groups in PDDAC was suggested.

Carbon nanoparticle materials were also used as stabilizers for liquid|liquid interface to drive ion transfer processes electrochemically (MacDonald et al. 2007). These materials were demonstrated to help emulsion microdroplets of organic liquids to be deposited onto ITO/glass electrode surface. Carbon nanoparticle materials with active surface area catalyzed the electron transfer and ion transfer process at triple phase boundary junction. In this study, it was suggested that CNP materials can be employed in the design of liquid|liquid interface or for modified electrode surfaces in electroanalytical applications.

In another work, CNP materials were codeposited on ITO/glass substrate electrode employing a sol-gel technique (Macdonald et el. 2008). It was shown that CNPs formed micrometer-sized aggregates in the presence of added salt. The presence of CNPs in the hydrophilic silicate film substantially extended the electrochemically active silicate film and its effect on double layer charging, solution phase processes with both reversible and irreversible heterogeneous electron transfer and heterogeneous three phase junction of electrochemical oxidation tert-butylferrocene suggested that incorporation of conductive CNPs with high surface area in functionalized sol-gel silicas could be an effective way for preparation of future sensors.

1.6.3 Gold nanoparticles

Gold nanoparticles are the most intensively studied and applied metal nanoparticles in electrochemistry due to their stable physical and chemical properties, useful catalytic activities and small dimension size (Daniel et al. 2004). These attractive properties allow them providing some

important functions for electroanalysis and construction of electrochemical sensors (Katz et al. 2004). Here, there is a short overview of application of these materials in electroanalysis.

After the wide use of colloidal gold in electron microscopy (Horisberger 1981), these materials were applied in sensing xanthine by adsorption of enzyme on colloidal gold (Crumbliss et al. 1992). Films were prepared by evaporation or electrophoretic deposition of xanthine oxidase on gold nanoparticles on the glassy carbon electrode. As a submonolayer of these particles covers the glassy carbon electrode, the modified electrode is stable only for a week. To solve this problem, gold nanoparticles were stabilized in an aminosilicate sol and then the electrodeposition occurs from this gold sol (Bharati et al. 1999 and 2001). The resulting film consists of gold nanoparticles covered with aminosilicate layer in which the amine group is locked onto the gold surface. It is possible to dope an enzyme to this system by simply adsorption of enzyme on gold sol (Bharati et al. 2001). The silicate matrix was served as the backbone for the enzyme (glucose oxidase), and the gold nanoparticle was an electrocatalyst for the oxidation/reduction of hydrogen peroxide. Both the oxidation and reduction of H_2O_2 as the by product of the enzymatic reaction can be monitored. The good stability and operation was obtained using this method for glucose measurement.

Using silver enhanced gold nanoparticles, an electrochemical assay for sequence specific DNA analysis was developed (Cai et al. 2002). Silver enhancement was used by forming shells of silver around gold particles to amplify the signal. This sensor was based on the electrostatic adsorption of targets which were oligonucleotides onto the modified glassy carbon electrode and hybridization was occurred onto gold labeled probe. This research showed the gold nanoparticle labeling with silver enhancement holding great promise for DNA hybridization electroanalysis in future.

Gold nanoparticles were immobilized on cystamine-modified gold electrode to make an array for sensing dopamine in the presence of ascorbate (Raj et al. 2003). This nano-Au electrode demonstrated good sensivity and selectivity against ascorbic acid and antifouling properties. The schematic representation of this electrode preparation is shown in Figure 3.

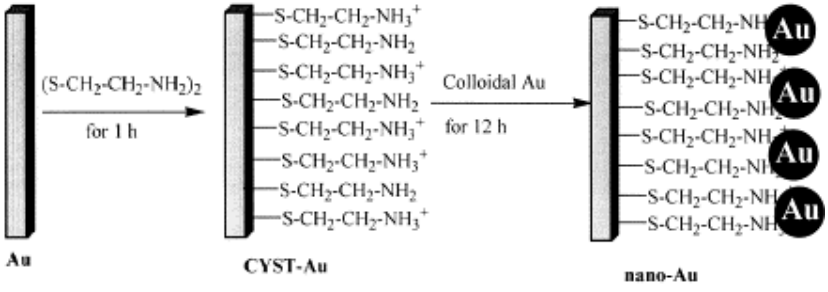

Figure 3. Schematic representation of the fabrication of the nano-Au self-assembly (note that this is a pictorial representation and is not on the correct scale) (Raj et al. 2003) (with kind permission from Elsevier).

In another work, a DNA membrane was electrodeposited on glassy carbon electrode and then gold nanoparticles were deposited on the surface of DNA layer to build a hybrid device of nanoscale sensor for norepinephrine measurement in the presence of ascorbic acid (Lu et al. 2004). The reversibility of the electrode oxidation reaction of norepinephrine was significantly improved and 200 mV negative shift in peak potential and also a large increase in peak current was observed for this system. That the electron transfer for oxidation of both ascorbic acid and norepinephrine is a surface adsorption controlled process was another advantage of this electrode.

A gold nanoparticle based potentiometric immunosensor was developed for detection of hepatitis B surface antigen (Tang et al. 2004). In brief, the Nafion with $-SO_3^-$ group was immobilized on a platinum disk electrode surface to absorb the $-NH_3^+$ in antibody molecules by electrostatic attraction. Then, the gold nanoparticles and hepatitis B surface antibody were entrapped by a gelatin matrix on the Nafion film surface. In contrast to common methods, this technique let antibodies immobilize with a higher loading amount and better retained immunoactivity on the electrode surface.

A hydrogen peroxide sensor based on the peroxidase activity of hemoglobine was prepared on gold nanoparticle-modified ITO/glass electrode (Zhang et al. 2004). The gold nanoparticles grew on ITO/glass electrode by a surfactant assisted seeding approach. Then this electrode was immersed in hemoglobine (Hb) solution to prepare Hb/Au/ITO/glass electrode. The Hb immobilized gold nanoparticle modified ITO/glass electrode exhibited an effective catalytic response to reduction of H_2O_2 with good reproducibility and stability. The reason for this behavior was related to the promoted electron transfer of Hb by gold nanoparticles.

Gold amalgam nanoparticle modified glassy carbon electrode was used for heavy metal measurement (Welch et al. 2004). In order to prepare this electrode, gold nanoparticles were deposited on glassy carbon electrode and then this electrode was used as substrate for mercury electrodeposition to create gold amalgam electrode. It was found that this electrode possessed higher sensitivity towards oxidation of Cr(III) to Cr(IV) species compared to gold macroelectrodes. This behavior suggested the possible application of gold nanoparticles as electrode materials for determination of heavy metals. In another study, the gold nanoparticles were electrodeposited onto a disposable screen printed electrode via an electrodeposition step to be used a sensor for environmental monitoring (Liu et al. 2007). This electrode was proved to have strong adsorption towards Cr(VI) species which results in an enhanced reduction current of Cr(VI). The performance of this sensor was evaluated with river water samples spiked with Cr(VI).

For arsenic (III) determination, gold nanoparticle modified glassy carbon electrode was developed (Dai et al. 2004). Gold nanoparticles were deposited onto glassy carbon electrode from chlorauric acid ($HAuCl_4$) solution. After use of this electrode in arsenic (III) solution, the results suggested the possible use of this method for the field screening of natural waters considering Cu as the only likely interference. In another work, Cu interference in arsenic (III) measurement was investigated for both a gold macroelectrode and gold nanoparticle modified electrodes (Dai et al. 2005). It was shown that the sensitivity of gold nanoparticle modified basal plane pyrolytic graphite (BPPG) electrode was 10 times and for gold nanoparticle modified glassy carbon electrode 3 times more than a gold macroelectrode. It was shown that gold nanoparticle modified electrodes can reduce the interference by Cu (II) for As(III). A lower detection limit was obtained for gold nanoparticle modified electrodes.

By covalent attachment of glucose oxidase (GOx) to a gold nanoparticle modified Au electrode, a biosensor was prepared for glucose sensing (Zhang et al. 2005). The assembled gold nanoparticles can facilitate electron transfer between analyte and electrode surface, also increase the enzyme loading, and have low effect on enzyme activity. Development of this electrode with improved surface coverage and high sensitivity was proposed as an important step towards miniaturization of sensors.

Gold nanoparticles/titania sol-gel composite membrane was prepared on glassy carbon electrode and applied as an immunosensor (Chen et al. 2006). This membrane can encapsulate the horseradish peroxidase labeled hCG antibody (HRP-anti-HCG) in the composite architecture and could be used for reagentless electrochemical immunoassay. To prepare this electrode, colloidal gold nanoparticles was mixed with HRP-anti-hCG. After dropping an aliquot of this solution on GCE surface, titanium isoperpoxide was immobilized on this electrode surface. The presence of gold nanoparticles provided a congenial microenvironment for adsorbed biomolecules and decreased the electron transfer impedance, leading to a direct electrochemical behavior of the immobilized HRP.

A gold nanoparticle/alkanedithiol conductive film on gold electrode surface was prepared for determination of catechol as an environmental pollutant (Su et al. 2006). Self assembled monolayer of alkanedithiols $HS(CH_2)_nSH$ (n=3,6,9) were prepared by immersing the Au electrode into ethanol solution containing $HS(CH_2)_nSH$. The prepared gold nanoparticle SAM modified electrodes possessed excellent electrode activity without a barrier for heterogeneous electron transfer between the bulk Au and redox species in solution phase. This demonstration provided a new platform for electrochemical investigations and electroanalytical applications such as electroanalysis of trace amount of environmental pollutants.

A voltammetric sensor for epinephrine (EP) was developed with a novel method from fabrication of gold nanoparticles with the dithiothreitol (DTT) and dodecanethiol (DDT) mixed self assembled approach (Wang et al. 2006). The mixed self assembled monolayers were first formed by the assembly of DTT and DDT from solution onto gold electrode. When these thiol rich surfaces were exposed to Au colloid, the sulfurs form strong bonds to gold nanoparticles anchoring the clusters to the electrode surface and a new nanogold electrode surface was obtained. This electrode was shown to promote the electrochemical response of EP by cyclic voltammetry.

A sensitive immunosensor for detection of pregnancy marker was developed using the direct electrical detection of gold nanoparticles (Idegami et al. 2007). A disposable screen printed carbon strips was used for the development of this probe. Simply, after the recognition reaction between the immobilized primary antibody and hCG, the captured antigen was sandwiched with a secondary antibody which was labeled with Au nanoparticles. This immunosensor system providing a combination of the screen printing technology with gold nanoparticles suggested a promising biosensor for different applications in electroanalysis.

It seems gold nanoparticle modified electrode surfaces can be prepared in three ways, by binding gold nanoparticles with functional groups of self assembled monolayers (SAMs), by direct deposition of nanoparticles onto the bulk electrode surface, and by incorporating colloidal gold into the electrode by mixing the gold nanoparticles with other components in the composite electrode matrix (Yáňez-Sedeňo et al. 2005). These materials have been extensively used as an immobilized

matrix for retaining the bioactivity of macromolecules such as proteins and enzymes and promoting the direct electron transfer of the immobilized proteins.

1.7 Research Motivation

Nanomaterials have been attractive subjects in all fields due to their exceptional properties compared to bulk materials. It is possible to change their size and shape and manipulate them with different materials to prepare a broad range of nanostructures with different physical and chemical properties. In this regard, many methods have been investigated to fabricate novel nanostructures for different purposes.

Electroanalytical chemistry is a field of science where researchers utilize the relationship between chemical phenomena involving charge transfer and electrical properties that accompany these phenomena for some analytical determination. In order to achieve high sensitivity or selectivity in electrochemical analysis, three major factors drew the particular interests. The three factors are electrode material, electrode geometry, and the detection method. All these three factors have been popular research topics in electrochemical analysis. For example, for heavy metal detection, researchers initially found the dropping mercury electrode, and step by step it was replaced with thin film mercury electrode and then carbon electrodes due to high toxicity of mercury. With the commence of nanotechnology revolution in all fields, nanomaterials with unique properties and potential technological applications have been used widely as electrode materials for different purposes such as sensor devices, fuel cells, and capacitors as discussed in previous parts.

Although different nanomaterials have been widely used in electroanalysis in recent years, less attention has been paid to new nanomaterials such as carbon nanofibers and carbon nanoparticles in electroanalysis and only a few works have been reported so far. In this regard, the aim of the present work was to study and develop new thin film electrodes based on new nanomaterials for electroanalytical purposes. These materials were used for new sensor design with a variety of techniques. After preparation, these films were studied with electronic microscopes to get better understandings of their morphology or their thickness. Then, cyclic voltammetry experiments helped to get information about their electrochemical behaviors. Finally, the possible applications of these electrodes were suggested.

2. Experimental

2.1 Chemical reagents

The main materials used in this study to modify the electrode surfaces were three different types of Pyrograf III carbon nanofiber from Pyrograf Product Inc. (**I**), Phenylsulfonate surface functionalized carbon nanoparticles from Cabot Corporation (**II** and **III**), Octakis (tetramethyl ammonium) pentacyclo-[9.5.1.13,9.15,15.17,13]-octasiloxane-1,3,5,7,9,11,13,15-octakis (yloxide) hydrate or poly-silsesquioxane silicate (PSS) and ruthenium(**V**) chloride ($RuCl_3$) from Sigma and Verton, respectively (**V**), and colloidal gold nanoparticles with 5 nm diameter from Sigma-Aldrich (**IV**).

2.2. Instrumentation

A microAutolab III potentiostat system (EcoChemie, Netherlands) was employed for voltammetric studies with a saturated calomel reference electrode (Radiometer, Copenhagen) and a platinum gauze counter electrode. Different electrode materials were used directly or as substrates for modified electrodes to prepare working electrodes. Here, the common electrode materials used in the present research are introduced.

1. Indium tin oxide electrode: Indium oxide doped with tin oxide (ITO) is used to make transparent conductive coatings. ITO coated glass is tin-doped indium oxide films which sputter-coated onto glass. In all experiments, the ITO/glass active surface area was 10 mm × 10 mm (**II** and **V**). The ITO/glass electrodes were rinsed with acetone and water, and then heat treated in a tube furnace for one hour at 500 °C, and re-equilibrated to ambient conditions before use. These materials were obtained from Image Optics, Basildon, UK.

2. Boron doped diamond electrode: A rectangular rod boron-doped diamond electrode was mounted in epoxy (a thin layer of Torrseal^{TM} ceramic epoxy and two-component epoxy E14A and E14B mounted into a 5 mm outer diameter borosilicate glass tube (**IV**).

3. Glassy carbon electrode: In all experiments, a 3 mm glassy carbon electrode (GCE) was used (**I** and **III**). This electrode was polished with 0.3 alumina slurries on the polishing pad and then sonicated in distilled water before use.

2.3 Characterization methods

In order to characterize the prepared nanostructured composites on the electrode surfaces various methods were used including:

2.3.1 Scanning electron microscopy

A JEOL JSM6310 system was applied for all SEM experiments. These experiments were carried out for carbon nanofiber poly styrene electrode, PSS – Ru^{3+} composite films on ITO/glass, and gold nanoparticle modified boron doped diamond electrode. In order to make surface more conductive, all samples (**I, III,** and **V**) were gold sputter coated for 30 s prior to taking images. This helps to make the surfaces conductive.

Gold nanoparticle modified boron doped diamond electrode (**IV**) was carbon sputter coated before SEM experiments.

2.3.2 Atomic force microscopy

Atomic force microscope images were obtained with a Digital Instruments Nanoscope IIIa MultiMode Scanning Probe Microscope in the AFM contact mode. AFM experiments were done for layer by layer thin film electrodes in the AFM contact mode (**II** and **V**). These experiments were employed to image the progress of the deposition process and to obtain information about uniformity of the process. The films were scratched with a scalpel prior to imaging in order to expose the substrate.

2.4 Nanoassembly methods

There are different methods used for preparation of nanostructured materials on the electrode surfaces in order to modify them such as:

2.4.1 Electro-aggregation technique: Electro-aggregation or electric field induced aggregation of interfacial colloid was used to prepare porous high surface area gold film on the boron doped diamond substrate electrode **(IV)**. A boron doped diamond electrode and a platinum wire were placed in a partially destabilized colloidal gold solution and then a potential of -5.0 V for different times was applied between them.

2.4.2 Layer by layer assembly technique: Layer by layer assembly technique developed by Decher (Decher 1997), here, was used to prepare two different structured thin films on ITO/glass electrode.

In order to prepare PSS – Ru^{3+} composite films (**V**), a solution of $Si_8O_{20}^{8-}$ and a solution of $RuCl_3$ both in ethanol were prepared separately. For deposition to occur, the ITO/glass electrode was dipped first into the $RuCl_3$ solution for 20s and then rinsed with ethanol and dried, and then it was dipped into silicate solution for 20s, rinsed with ethanol and dried. This procedure was repeated to build up multi-layer films.

In order to prepare chitosan-carbon nanofiber films at ITO/glass electrode, an aqueous suspension of carbon nanoparticle and a solution of chitosan were prepared separately (**II**). For deposition to occur the ITO/glass electrode was dipped first into the carbon nanoparticle solution for 30 s, rinsed

with water and then it was dipped into chitosan solution for 30 s, and rinsed with water. This procedure was repeated to build up multi layer thin film electrode.

2.4.3 Solvent evaporation technique: For carbon nanoparticle chitosan thin film preparation on glassy carbon electrode, a solution of carbon nanoparticle chitosan was prepared **(III)**. Then, an aliquot of this solution was dropped on glassy carbon electrode and let it evaporate in oven. The uniform black thin film was obtained on glassy carbon electrode.

2.4.4 Thermal-compression formation: This method was used to prepare carbon nanofiber poly styrene electrode (**I**). In order to prepare this electrode, a suspension of carbon nanofiber and polystyrene in toluene was evaporated to leave a black solid composite. This composite was mechanically grounded, and it was heated in a pellet press both in air and vacuum, respectively, in an oven. Then, a force of 50 N was applied to this hot pellet press and it was allowed to be cool down under mechanical pressure. The resulting pellet was back contacted to a copper wire with silver epoxy and mounted in epoxy. The pellet electrodes had a 3 mm diameter and approximately 1 mm depth and it could be simply repolished for surface renewal. Figure 2 represents a schematic of this electrode design.

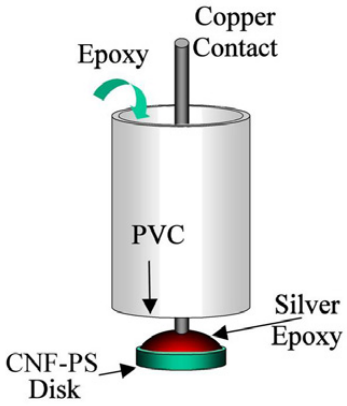

Figure 1. Schematic drawing showing the carbon nanofiber polystyrene electrode assembly process.

3. Results and discussion

3.1 Carbon nanofiber-polystyrene composite electrode for electroanalytical processes (I)

The development of composites based on conductive carbon phases dispersed in polymeric matrices has led to important advances in analytical chemistry and sensor devices. These new materials combine the electrical properties of graphite with the ease of processing of plastics and show attractive electrochemical, physical, mechanical, and economical features (Céspedes et al. 1996). As carbon nanofiber materials provide active and well-defined high surface area materials for electrochemical processes, here, a novel procedure is suggested for preparation of CNF electrodes (diameter 3 mm) with a PS binder for electroanalytical purposes.

Three types of Pyrograf III carbon nanofibers, some of which have been high-temperature graphitized and some have been produced with a very low iron impurity level, and a range of carbon nanofiber to polystyrene compositions were prepared and highly electrically conducting and re-newable CNF-PS composite electrodes were obtained with a 33wt% carbon nanofiber in polystyrene. Low carbon nanofiber content pellets (20%wt carbon nanofiber) resulted in very high electrical resistance and high carbon nanofiber content (50 wt %) resulted in more porous electrode materials.

Figure 1A shows a typical SEM image of the carbon nanofiber material and in Figure 1B an electrode with high porosity (50%wt CNF) is shown. A typical image of a 33 weight% carbon nanofiber– polystyrene electrode is presented in Figure 1C. This kind of electrode surveys the most promising results and it could be re-used after re-polishing the electrode surface.

CNF-PS disk electrodes were initially characterized by voltammetric measurements in aqueous 0.1 M KCl containing 1mM $Ru(NH_3)_6^{3+}$ in compare to glassy carbon electrode. First a potential range was chosen where only capacitive currents are recorded. Due to the polystyrene matrix, the capacitive current for carbon nanofiber-polystyrene electrodes is considerably decreased. Figure 2 shows the results obtained for this electrode in the mentioned solution.

In the presence of a reversible redox system, $Ru(NH_3)_6^{3+}$, a well defined voltammetric reduction–reoxidation response is observed at -0.19 V vs. SCE. Compared to glassy carbon, the reduced faradic peak currents can be attributed to partial diffusion domain blocking of the electrode surface due to polystyrene. The density of carbon nanofibers exposed at the electrode surface is too high for individual independent diffusion zones to form and therefore steady state characteristics are not observed. For different types of Pyrograf III carbon nanofibers, similar characteristics such as low capacitive background current are observed as it is shown in Table 1.

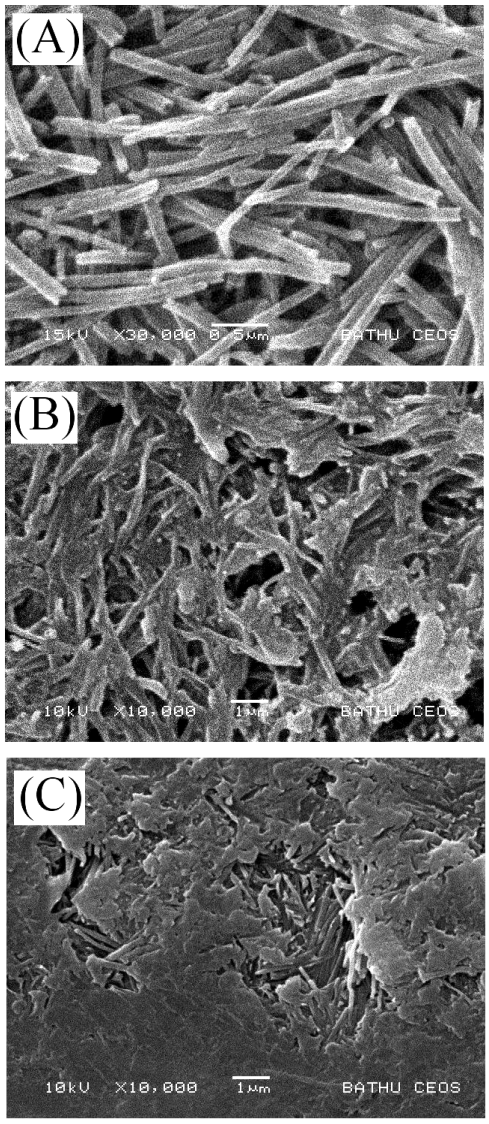

Figure 1. SEM images for (A) carbon nanofiber material, (B) a porous 50 weight% carbon nanofiber – polystyrene electrode, and (C) a 33 weight% carbon nanofiber– polystyrene electrode.

Table 1. Voltammetric data (scan rate 0.1 Vs^{-1}) obtained for different types of CNF-PS electrodes immersed in 1 mM Ru $(NH_3)_6^{3+}$ in aqueous 0.1 M KCl.

Electrode	Capacitive current / µA	Capacitance / 10^{-9} Farad	I_p^{red} / µA	I_p^{ox} / µA
33% PR-24-XT-PS	1.5×10^{-2}	75	16	13
33% PR-24-XT-HHT	3×10^{-2}	150	14	12
33% PR-24-XT-LHT	3×10^{-2}	150	16	14
GC	0.6	3000	33	31

The ability of the CNF-PS electrode to act as an analytical sensor has been explored in Pb^{2+} determination in aqueous media. The uniformity of the surface reactivity of CNF-PS electrode towards Pb metal deposit has been investigated by SEM and it becomes clear that nucleation at the carbon nanofiber surface is facile and simultaneous under the employed conditions.

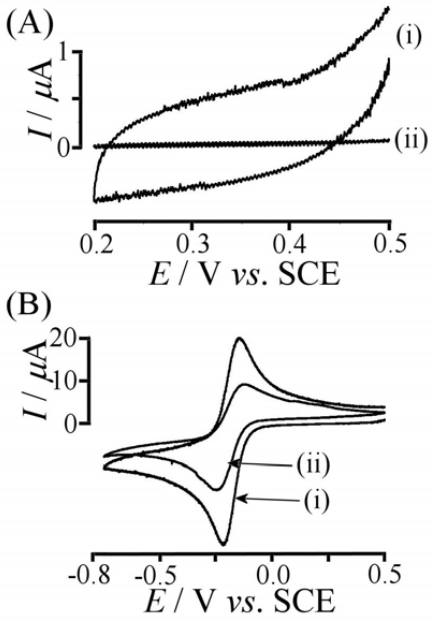

Figure 2. Cyclic voltammograms obtained in 1 mM $Ru(NH_3)_6^{3+}$ in aqueous 0.1 M KCl. (A) Cyclic voltammograms (scan rate 0.1 Vs^{-1}) obtained with (i) a 3 mm diameter glassy carbon electrode and (ii) a 3 mm diameter CNF-PS electrode (33% PS). (B) Cyclic voltammograms (0.1 Vs^{-1}) obtained with (i) a 3 mm diameter glassy carbon electrode and (ii) a 3 mm diameter CNF-PS electrode (33% PS).

The possibility of incorporating an additive to this electrode was shown by depositing 1,1´-ferrocenedicarboxylic acid onto carbon nanofibers and embedding into the CNF-PS electrode. These electrodes with immobilized 1,1´-ferrocenedicarboxylic acid reveals a new anodic peak

when immersed in 0.1 M KCl solution. As most of the oxidized 1,1´-ferrocenedicarboxylic acid is dissolved from electrode surface into the aqueous solution, the corresponding cathodic peak is small and hard to recognize. Therefore, it is clear that it is possible to incorporate other reagents for electroanalytical purposes such as metal accumulation.

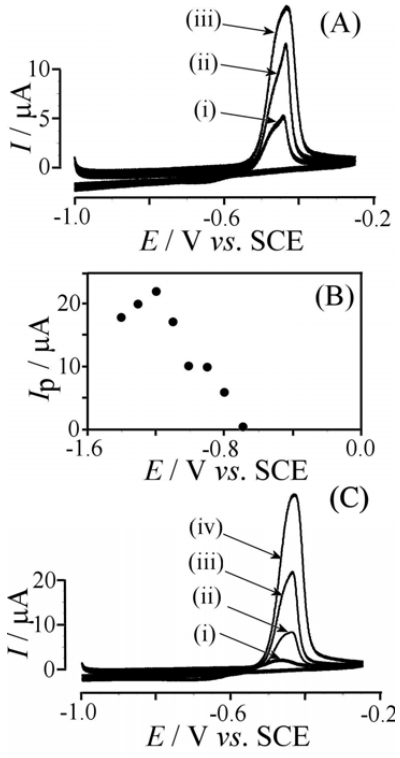

Figure 3. (A) Anodic stripping voltammograms (scan rate 0.1 Vs-1, deposition at -1.2 V vs. SCE, deposition time 500 s) obtained with a 3 mm diameter CNF-PS electrode (33% PS) immersed in 10 μM Pb^{2+} in 0.1 M HNO_3. (B) Plot of the peak current observed for the anodic stripping voltammogram versus the deposition potential (other conditions as in (A)). (C) Anodic stripping voltammograms (scan rate 0.1 Vs^{-1}, deposition at -1.2 V vs. SCE, deposition time 500 s) obtained with a 3 mm diameter CNF-PS electrode (33% PS) immersed in (i) 2 (ii) 10 (iii) 20 (iv) 40 μM Pb^{2+} in 0.1 M HNO_3.

In conclusion, a new type of electrode has been prepared by embedding carbon nanofibers in a thermoplastic polystyrene matrix. Well voltammetric characteristics with low electrical resistance and capacitance were obtained and the electrode was tested for detection of Pb^{2+} aqueous solution. This type of analytical electrode is easily repolished, cheap, and convenient for electroanalytical use.

3.2 Chitosan-Carbon Nanoparticle Film Electrodes: Physisorption versus Chemisorption (II and III)

Carbon materials are widely used in electroanalysis (Safavi et al. 2006) and recently the benefits of nanocarbon materials has been a trigger of new developments in the design of new electrodes for electrochemical sensing. The use of chemically surface-modified (tosylated) carbon nanoparticles with negative surface charge in layer by layer assembly of thin carbon films has been reported recently for the polycationic binder poly(diallyldimethylammonium chloride).

Here, thin chitosan-carbon nanoparticle films are prepared both in layer by layer assembly from separate aqueous solutions giving typically 20-200 nm films on ITO/glass electrode and by solvent evaporation of aqueous solutions giving typically 100 nm per layer on glassy carbon substrates. In both films, chitosan introduces amine/ammonium functionalities for redox active probes and the composition of film is controlled by varying the chitosan content during assembly. Chitosan is also a binder for mesoporous carbon nanocomposite structure in layer by layer formation.

The film formation methods provide electrochemically stable and active films ready for immobilization of redox systems for physisorption of indigo carmine and chemisorption of 2-boromethyl-anthraquinone to the active sites.

3.2.1 Formation and electrochemical characterization of carbon nanoparticle thin film electrodes: Layer-by-layer thin films vs. solvent evaporated film

The layer by layer formation of a very thin film is confirmed by change in colour from clear to black on ITO/glass electrode during deposition and by AFM images. These images confirm the uniformity of the film and reproducibility of its formation. Figures 4 A-C show the AFM images of layer by layered carbon nanoparticle chitosan film on ITO/glass substrate.

Composite films of chitosan and carbon nanoparticles are also formed when an aqueous solution containing both components is dried onto a substrate. Electron microscopy images of these films demonstrate the uniformity on microscopic level of the dry films. From these images, an average increase of ca. 2 nm in each carbon nanoparticle deposition cycle can be estimated. Figures 4 D-F present the SEM images for carbon nanoparticle chitosan solvent evaporated films on glassy carbon electrode. These images demonstrate the uniformity on the microscopic level and the average thickness of ca. 100 nm increase per layer.

In compare to layer by layer deposited film, the preparation of solvent evaporated film is faster and more reproducible. The electronic properties of both film electrodes were explored with cyclic voltammetry in 0.1 M phosphate buffer and a linear capacitance contribution from the carbon nanoparticle deposit with the increase of number of layers was observed during deposition.

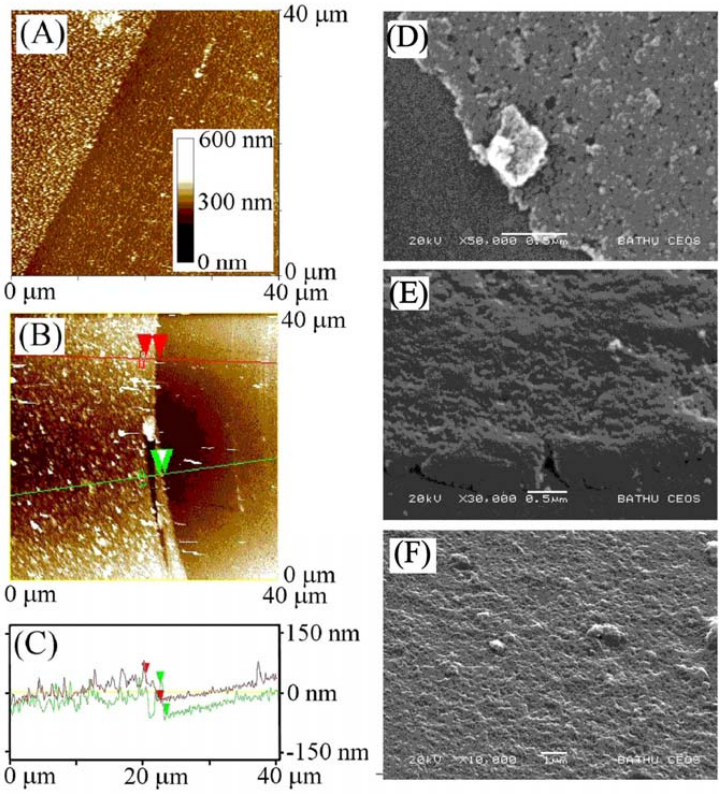

Figure 4. Left: AFM images of (A) 20 layer carbon nanoparticle chitosan film, (B) a 40 layer carbon nanoparticle chitosan film, and (C) Cross-sectional height analysis. Right: SEM images for (D) one (E) two, and (F) a four layer carbon nanoparticle chitosan deposit. All samples were scratched with scalpel revealing the underlying substrate.

3.2.2 Physisorption of a model redox system (Indigo carmine): Layer-by-layer thin films vs. solvent evaporated film

The structure of chitosan is strongly affected by the presence of the amine functionality which remains protonated over a wide range of proton activities. The positive charge introduced by ammonium is responsible for its reactivity towards hydrophobic anions.

Indigo carmine, a well-known reversible 2 electron-2 proton redox system, has been applied as a negatively charged redox system to probe the chitosan binding sites via physisorption to carbon nanoparticle-chitosan thin films. The electrochemical properties of the indigo carmine physisorbed into the chitosan-CNP film electrode are dominated by the state of protonation of the glucosamine

functionality. After indigo carmine immobilized into the film, the electrode was transferred to into clean phosphate buffer solution for electrochemical investigation.

The adsorbed redox system was observed as a reversible response at - 70 mV vs. SCE in phosphate buffer pH 2 for layer by layer film and at - 90 mV vs. SCE for solvent evaporated film. The voltammetric response is linearly dependent on the number of layers applied during thin film formation for both films, but an apparent transition is supposed to be observed for both films at higher number of layers due to a diffusion effect.

For layer by layer film, the peak current is increasing proportionally with scan rate consistent with a thin layer of fully active redox material immobilized at electrode surface. While in solvent evaporated film, the shape of the voltammetric peaks is scan rate dependent and a log-log plot of the peak current versus the scan rate with a transition from thin film to thick film due to proton diffusion was observed as it can be seen in Figure 5.

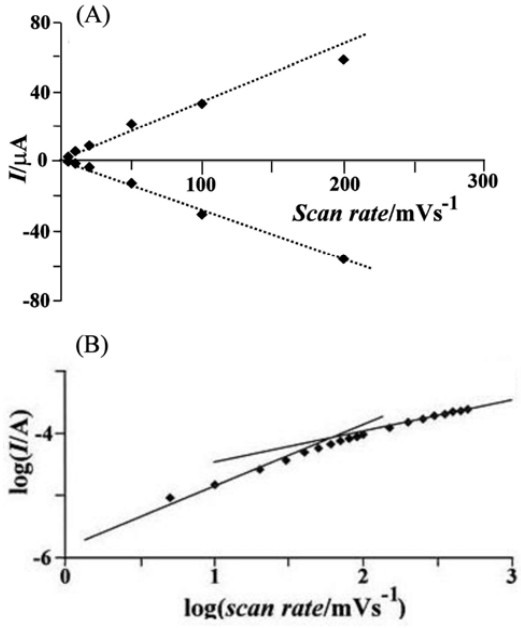

Figure 5. (A) Plot of the peak current versus scan rate for a 10 layer carbon nanoparticle chitosan film on ITO immersed in 0.1 M phosphate buffer pH 2. (B) Log-Log plot of peak current for oxidation of indigo carmine versus the scan rate with lines indicating slopes 1.0 and 0.5 for solvent evaporated film on glassy carbon electrode. (The indigo carmine was immobilized on the electrode by immersion into 1mM indigo carmine in 0.1 M phosphate buffer pH 2.)

For carbon nanoparticle chitosan, multi layer film on ITO/glass electrode, the effect of the solution pH on voltammetric response shows a typical cyclic voltammograms for the reduction and re-oxidation of indigo carmine at pH 2, 3, and 4 and a shift of midpoint potential to more negative values occurs at lower proton activity consistent with the Nernstian shift expected for the indigo

carmine redox system. Furthermore, the shape of the voltammetric response is changing and broader signals are observed as the pH is increased and no voltammetric signals for indigo carmine reduction are observed at pH>6 because of the loss in positively charged ammonium binding sites for indigo carmine.

In the case of solvent evaporated film on glassy carbon electrode, an approximately Nernstian shift in the mid point potential with pH is observed and decrease in peak current at more alkaline conditions is also demonstrated (Figure 6).

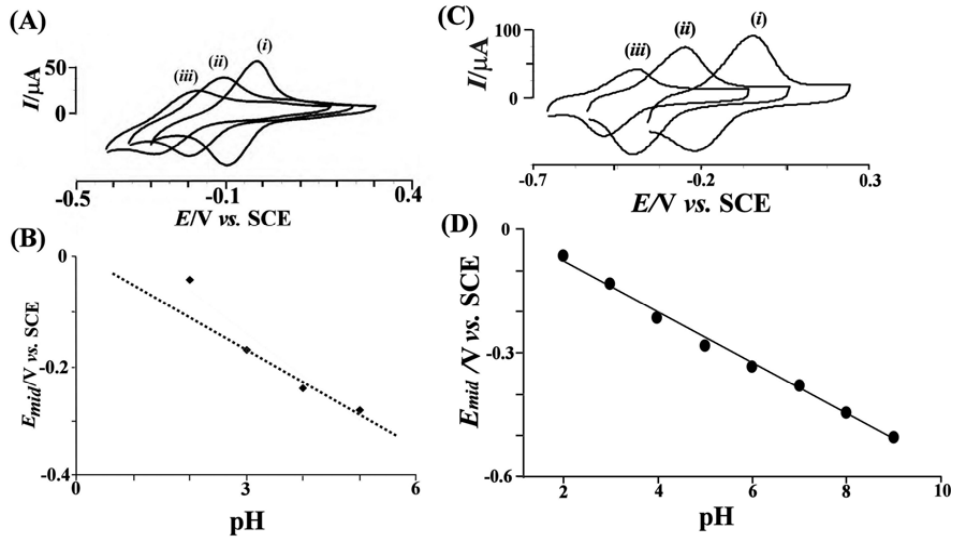

Figure 6. (A) Cyclic voltammograms (scan rate 0.1 Vs^{-1}, area 1 cm^2) for a 10 layer chitosan-CNP film electrode (pretreated in 1 mM indigo carmine in 0.1 M phosphate buffer pH 2), see experimental in paper immersed in 0.1 M phosphate buffer at pH (i) 2, (ii) 3, and (iii) 4. (B) Plot of the mid point potential E_{mid}=1/2 (E_p^{ox}+ E_p^{Red}) for reduction and re-oxidation of indigo carmine in immobilized in a 10-layer chitosan-CNP film versus the pH in 0.1 M phosphate buffer solution. (C) Cyclic voltammograms (scan rate 0.1 Vs^{-1}) for the reduction and reoxidation of physisorbed indigo carmine at a chitosan-CNP modified glassy carbon electrode in aqueous 0.1 M phosphate buffer at pH (i) 4, (ii) 8, (iii) 12. (D) Plot of the midpoint potential versus pH.

By varying the concentration of indigo carmine during the deposition step, the charge under the voltammetric peak can be changed and a plot of the anodic charge versus the indigo carmine concentration is shown in Figure 7. A clear transition in the peak current is observed at a concentration of approximately 100 μM indigo carmine when the binding ability of indigo carmine in to the chitosan-CNP was investigated for both films. The analysis of the langmuir plot suggests an approximate binding constant of $K_{indigocarmine} = 1.5 \times 10^4$ mol^{-1} dm^3 for layer by layer film and 3×10^4 $mol^{-1}dm^3$ for solvent evaporated film. The difference between these numbers can be referred to delayed diffusion in thicker film on glassy carbon electrode.

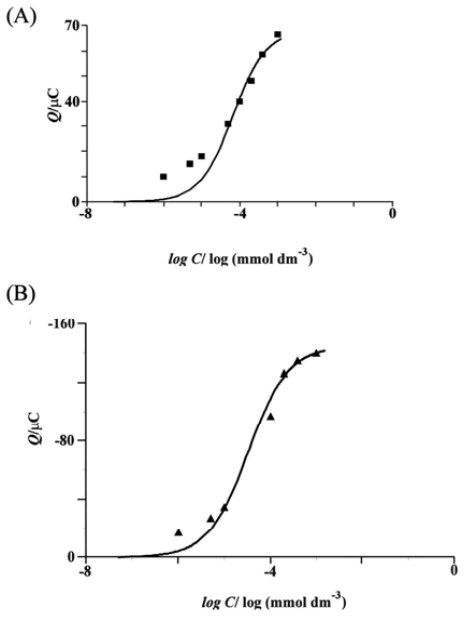

Figure 7. Langmuir isotherm plot for immobilization of indigo carmine physisorbed into a chitosan-carbon nanoparticle film. (A) For layer by layer film on ITO, the line corresponds to a binding constant $K_{indigocarmine}$ = 15000 mol^{-1} dm^3. (B) For solvent evaporated film, the line corresponds to a binding constant $K_{indigocarmine}$ = 30000 mol^{-1} dm^3.

In order to change the number of available binding sites, it is possible to change the chitosan concentration. The amount of chitosan within the layer by layer deposit can be altered by varying the concentration of chitosan during the deposition and a non-linear trend with an increasingly dramatic effect at lower chitosan concentration is observed. The amount of chitosan in the deposition mixture was varied in solvent evaporated film and it was observed that gradually decreasing the amount of chitosan results in a proportional change in peak current. It seems at low chitosan concentration in both cases, the present ammonium functional groups in chitosan bind to indigo carmine and therefore they are not available for physisorption and binding to carbon dominates.

3.2.3 Chemisorption of a model redox system (2-bromomethyl-anthraquinone): Layer-by-layer thin films vs. solvent evaporated film

The poly-glucoseamin structure in chitosan provides binding sites not only for physisorption but also for chemisorption. Here, 2-bromomethyl-anthraquinone has been applied to investigate the chitosan binding sites via chemisorption to carbon nanoparticle-chitosan thin films. Chemisorption of 2-methylene-anthraquinone can be achieved by a simple C-N coupling process in acetonitrile media. After the film was modified with 2-bromomethyl-anthraquinone, it was transferred into clean phosphate buffer solution for electrochemical investigation. The resulting methylene-

anthraquinone functionalization is readily observed in voltammograms recorded in aqueous phosphate buffer solution for both films and the process is highly stable with no indication of removal of redox centers from the electrode during prolonged redox cycling.

For both films, the effect of the solution pH on the voltammetric response for immobilized 2-bromomethyl-anthraquinone is considerably different from those observed for immobilized indigo carmine. The voltammetric signal is stable and a well defined shift in midpoint potential occurs with pH. The plot of the midpoint potential versus pH is consistent with Nernstian behavior over a broad range of pH. A minor inflection in the plot at pH 6-7 due to the deprotonation of chitosan is observed for multilayer film on ITO/glass electrode (Figure 8).

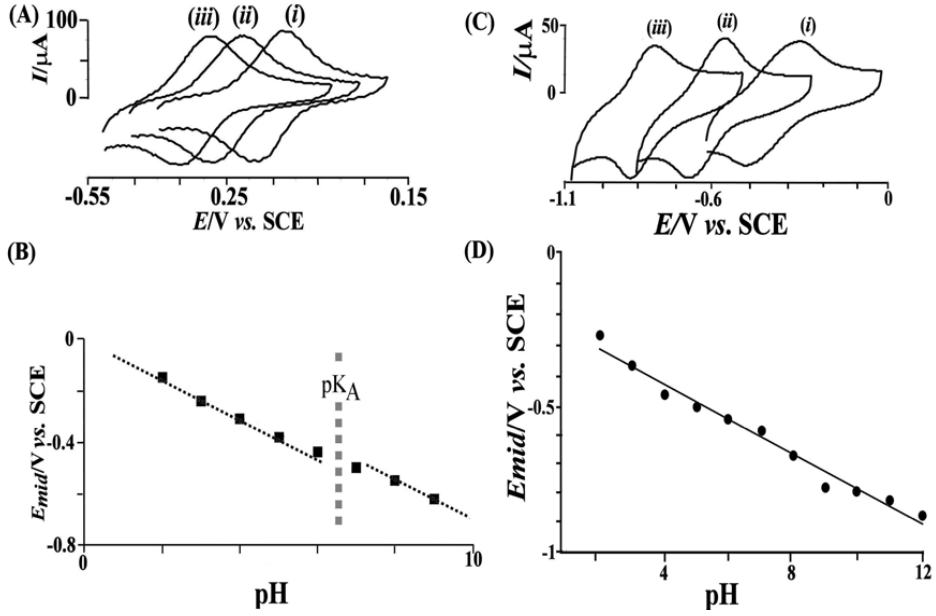

Figure 8. (A) Cyclic voltammograms (scan rate 0.1 Vs^{-1}, area 1 cm^2) for a 10 layer chitosan-CNP film electrode (pretreated in 1 mM 2-bromomethyl-anthraquinone in acetonitrile) immersed in 0.1 M phosphate buffer at pH (i) 2, (ii) 3, and (iii) 4. (B) Plot of the mid point potential E_{mid}=1/2 (E_p^{ox}+ E_p^{Red}) for reduction and re-oxidation of 2-methylene-anthraquinone immobilized in a 10-layer chitosan-CNP film versus the pH in 0.1 M phosphate buffer solution. (C) Cyclic voltammograms (scan rate 0.1 Vs^{-1}) for the reduction and reoxidation of chemisorbed methylene-anthraquinone at a chitosan-CNP modified glassy carbon electrode in aqueous 0.1 M phosphate buffer at pH (i) 4, (ii) 8, (iii) 12. (D) Plot of the midpoint potential versus pH. The effect of 2-bromomethylanthraquinone concentration during chemisorption process clearly shows a decrease in the amount of bound anthraquinone at lower 2-bromomethylanthraquinone concentration. From Figure 9, it can be observed that plot of the charge under the peak versus the concentration of 2-bromomethyl-anthraquinone shows typical Langmuir isotherm characteristics and a binding constant $K_{2\text{-bromomethyl-anthraquinone}}$ =1.9 ×10 ^{4} $mol^{-1}dm^3$ for layer by layer film and $K_{2\text{-bromomethyl-anthraquinone}}$ =1.4 ×10^4 mol^{-1} dm^3 for solvent evaporated film.

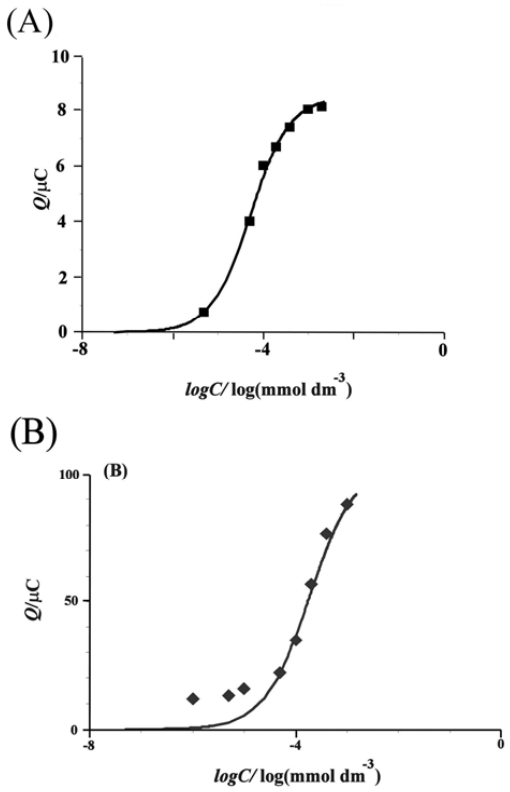

Figure 9. Langmuir isotherm plot for immobilization of 2-bromomethyl-anthraquinone chemisorbed into a chitosan-CNP film. (A) For layer by layer film, the line corresponds to a binding constant $K_{2\text{-bromomethyl-anthraquinone}}$ = 19000 mol^{-1} dm^3. (B) For solvent evaporated film, the line corresponds to a binding constant $K_{2\text{-bromomethyl-anthraquinone}}$ = 14000 mol^{-1} dm^3.

Changing the chitosan concentration during the deposition process shows a trend very similar to that observed for indigo carmine physisorption. Similar to physisorption, for layer by layer film, the scan rate effect on the peak current is consistent with a fully redox active thin film and for solvent evaporated film, the transition in scan rate is again assigned to proton diffusion or pH gradient.

Here, two different techniques have been employed to create thin film deposit of carbon nanoparticle on ITO/glass and glassy carbon electrode. The chitosan is shown to effectively bind and electrically connect the carbon film. By varying the chitosan concentration during deposition, the number of binding sites could be controlled. Therefore, it is possible to apply two different processes, physisorption and chemisorption, and creating multiple binding sites simultaneously where chemisorption provide special chemisorbed species with selectivity or structural constrains on the reactivity of the physisorbed redox system. So, it introduces the potential application of this effect for future chiral selection in electrosynthesis, or for enantioselective sensors.

3.3 Arsenite Determination in the Presence of Phosphate at Electro-Aggregated Gold Nanoparticle deposits (IV)

Different electrode materials have been used for arsenic determination but gold is the most suitable electrode material for arsenic measurement because of its high hydrogen overvoltage and better reversibility of the electrode reaction in both plating and stripping step (Forsberg, 1975). In this study, a new porous gold film on a boron doped diamond microelectrode surface is prepared by electro-aggregation and the reactivity of the electro-aggregated gold deposit towards arsenite is investigated in nitric media and in neutral phosphate buffer media.

The gold nanoparticle aggregation process is continuous and allows considerable deposits to be formed. SEM images show that the gold nanoparticle deposit is non-uniform and the deposition occurs preferentially on some diamond crystal surfaces and less on others (Figure 10).

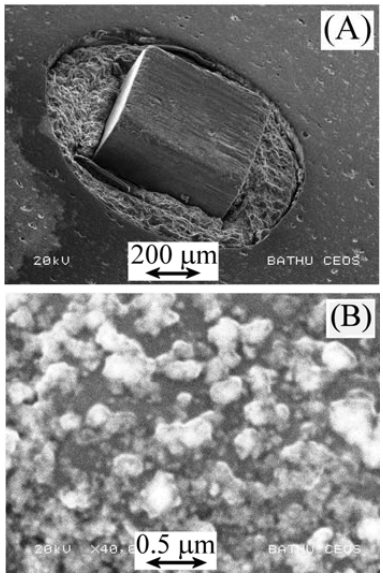

Figure 10. Scanning electron microscopy images of (A) a 500 µm boron-doped diamond electrode embedded in epoxy, (B) a high magnification image showing aggregates of 5 nm diameter gold nanoparticles at the boron-doped diamond surface (after 60 minutes deposition).

The reactivity of electro-aggregated gold nanoparticles was investigated in 10µM arsenite (III) in HNO_3. The deposition potential optimized as -0.6 V vs. SCE and it was shown that the stripping peak response is increasing with deposition time. Then, the effect of arsenic concentration on the analytical signal was demonstrated and a linear trend was observed when the charge under the stripping peak against the arsenite concentration was plotted. The increasing depth of gold nanoparticle aggregates and transport of reagents into mesoporous deposit cause a non-linear

increase with time. The submicromolar detection limits are readily achieved with this method in HNO_3 media. The detection limit in 0.1 M HNO_3 is 30 ppb.

The direct determination of arsenite in natural media of phosphate buffer was obtained for the electro-aggregated high surface area gold nanoparticle deposit with considerable sensitivity. A linear change was observed for reduction and oxidation response with arsenite concentration. The effect of the solution pH in the range of 3 to 11 shows a clear pH dependence of all voltammetric signals with approximately 58 mV per pH unit consistent with the Nernstian shift. The effect of the deposition time on the voltammetric signal shows that the anodic stripping response is improving with the increase in deposition time. The effect of the arsenic concentration shows two linear ranges with a switch in slope at 6 µM concentration. This behavior is characteristic for this monolayer deposition stripping process where the outer more accessible gold surface area is fully covered at relatively low arsenic concentrations (Figure 11).

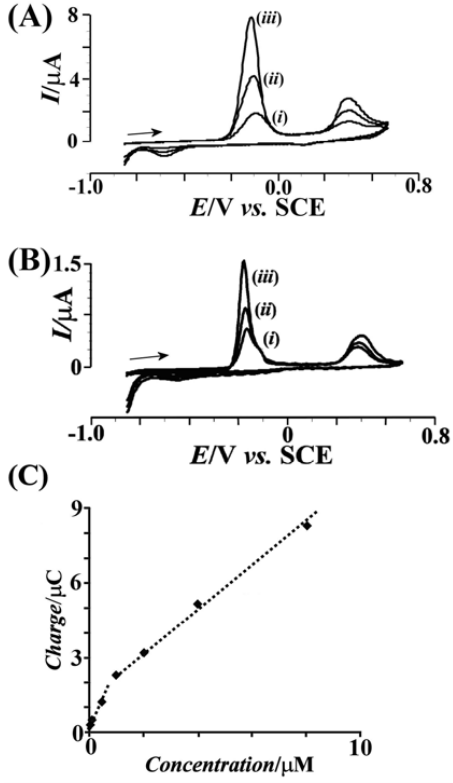

Figure 11. (A) Anodic stripping voltammograms (scan rate 100 mVs^{-1}, deposition at -0.8 V vs. SCE, deposition time 300 s, 30 minutes gold nanoparticle deposition) for (i) 10, (ii) 40, and (iii) 80 µM arsenite(III) in 0.1 M phosphate buffer pH 7. (B) Anodic stripping voltammograms (scan rate 100 mVs^{-1}, deposition at -0.8 V vs. SCE, deposition time (i) 50, (ii) 100, (iii) 200 s, for 30 min gold nanoparticle deposition) for 10 µM arsenite(III) in 0.1 M phosphate buffer pH 7. (C) Plot of the charge under the stripping peak for different concentrations of arsenite(III) in phosphate buffer pH 7.

In neutral phosphate buffer media, good analytical characteristics are observed and submicromolar detection limit for As (III) determination is easily obtained. The detection of limit obtained in neutral phosphate buffer is 1 ppb.

In this work, an electro-aggregated gold nanoparticle deposit on boron doped diamond electrodes is characterized. At this electrode the determination of arsenite (III) is possible even in phosphate buffer media at pH 7 with low detection limit.

3.4 Layer-by-Layer Assembly of Ru^{3+} and Octaanionic Silsequioxane into an Electrochemically Active Silicate Film (V)

The catalytic activity of ruthenium derivatives strongly depend on the oxidation state and on the reaction media used (Fachinotti et al. 2007) and they have been widely investigated in the field of electrocatalysis (Jirkovsky et al. 2006, Cao et al. 2006). The relatively low surface area of unsupported ruthenium oxides restricts catalytic applications and there have been considerable efforts to prepare highly porous supported ruthenium oxide electrodes. Excellent dispersion of ruthenium is possible on support materials like zeolite (Dutta et al. 2003), SiO_2 (Armelao et al. 2003), TiO_2 (Bavykin et al. 2005), and carbon (Mazurek et al. 2006). Organic functionalized mesoporous silicas represent a new class of materials for the design of catalysts, in particular because of high surface area, controllable pore structures and tailored pore surface chemistry which allows the binding of a large number of surface chemical moieties (Kuroki et al. 2002).

Here, layer by layer assembly method has been applied to form novel silicate films from octaanionic silsesquioxane and Ruthenium (III). The electrocatalytic behavior of hydrous ruthenium oxide embedded in the resulting silicate support on ITO/glass electrode surfaces is investigated.

AFM was employed to image the progress of the deposition process and to obtain information about uniformity. Initial stages of the film growth clearly show island formation and non-uniform growth but after 10 and more deposition cycles a steadily growing more uniform film is observed. Height measurements across scratched lines on the film allow the growth per deposition cycle to be estimated as 6 nm in average. SEM images obtained for the PSS-Ru^{3+} film show a uniformly porous film.

In order to characterize the PSS-Ru^{3+} film, electrochemical measurements were conducted in aqueous 0.1 M phosphate buffer solution. A reversible surface-immobilized redox system centered approximately at 0.1 V vs. SCE was revealed in cyclic voltammograms. The voltammetric peak increases linearly with both the number of deposited layers and the scan rate which is consistent with a surface immobilized redox system. From the charge under the peak, it can be estimated that only a small fraction of the ruthenium present in the film appears to be reacting. The electrochemical responses for different pH solutions show a systematic shift with pH by approximately 59 mV per pH unit for cyclic voltammograms and the PSS-Ru^{3+} film is chemically stable in the pH range from at least 1 to 9.

It seems that restructuring occurs during deposition process and very small nanoparticles of hydrous Ru_2O_3 embedded into a silicate matrix are formed during the deposition process. Impedance measurements show that increasing the number of layers of PSS-Ru^{3+} deposit is affecting mainly the charge transfer resistance and it can be rationalized with the increase in the surface concentration of the Ru (III) (-OH) (surface) species affecting the apparent exchange current density.

In order to investigate the reactivity of binding sites and obtain the additional estimate of the surface area and porosity of the PSS-Ru^{3+} film deposit, the methylene blue redox system with positive charge was chosen to be immobilized on this film. The cyclic voltammetric experiments in 0.1 M phosphate buffer solutions show a new redox process to be observed at -0.25 V vs. SCE. The experiments in different methylene blue concentrations show a weak dependence on concentration and therefore, the charge under the peak is not a well defined measure of surface area. As no color change of the adsorbed methylene blue occurs during potential cycling, it seems most of the adsorbed dye appears to remain electrochemically inactive in the film.

The UV-Vis spectroscopy of the immobilized methylene blue on PS-Ru^{3+} film shows that there is a nonlinear relationship between the absorption and film thickness and it may be because of the aggregation and the additional opaqueness of the film. These experiments also suggest a considerable increase in area for each deposition cycle which is consistent with high porosity and many binding sites for methylene blue on the silicate film, although it is electrochemically inaccessible. Figure 12 shows the effect of methylene blue concentration immobilized on PS-Ru^{3+} film and the UV-Vis data for methylene blue immobilized film.

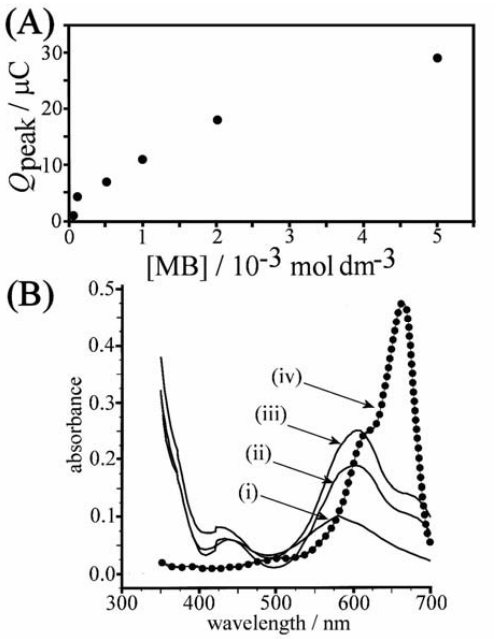

Figure 12. (A) Plot of the charge under the peak observed for the reduction of methylene blue on a 10-layer PS-Ru^{3+} electrode versus concentration of methylene blue in 0.1 phosphate buffer pH 7 immersion solution. (B) UV-Vis data for PS-Ru^{3+} films (i) 1 layer, (ii) 5 layers, and (iii) 8 layers (after 10 minute immersion in a 1 mM methylene blue solution in 0.1 M phosphate buffer pH 7 and rinsing with water) and (iv) a 8 μM methylene blue solution in 0.1 M phosphate buffer pH 7 in a 1 cm path length cuvette.

The hydroquinone-benzoquinone redox system was employed to further explore the reactivity of the related PSS-Ru^{3+} films. The oxidation of hydroquinone follows a 2 electron – 2 proton pathway and is known to be exceptionally slow on clean ITO/glass electrodes (Stott et al. 2006). It was observed that PSS-Ru^{3+} films even after only one layer deposition exhibited considerable electrocatalytic activity for the oxidation of hydroquinone. Both the oxidation of hydroquinone and the reduction of benzoquinone are catalyzed by the PSS-Ru^{3+} film when compared to bare ITO/glass. The effect of the number of deposition layers on the oxidation process shows an improvement for up to 10 layer deposits but the effect of PSS-Ru^{3+} thickness is not pronounced.

RuO_2 is known to catalyze the ceric-driven oxidation of arsenic (Gajic-Krstajic, 2004), therefore, PSS-Ru^{3+} film was applied for the electrocatalytic oxidation of AsO_3^{3-} to AsO_4^{3-} in the presence of phosphate.

Initial exploratory voltammetric experiments suggested that no significant electrocatalytic current occurs at potential negative of 0.5 V vs. SCE. However, when the potential is scanned positive of 0.5 V vs. SCE the onset of an anodic process is observed. Increasing the thickness of the PS-Ru^{3+} film increased current and the full potential range up to 1.5 V vs. SCE in spite of oxidation of the PS-Ru^{3+} film was explored. Figure 11A shows that the onset of a current response at 0.5 V vs. SCE is followed by a broad current peak at ca. 1.3 V vs. SCE which is indeed approximately correlated

to the concentration of arsenite(III) (Figure 13). Unfortunately, this oxidation process is irreversible and in a second and subsequent potential cycle the electrode is completely inactive.

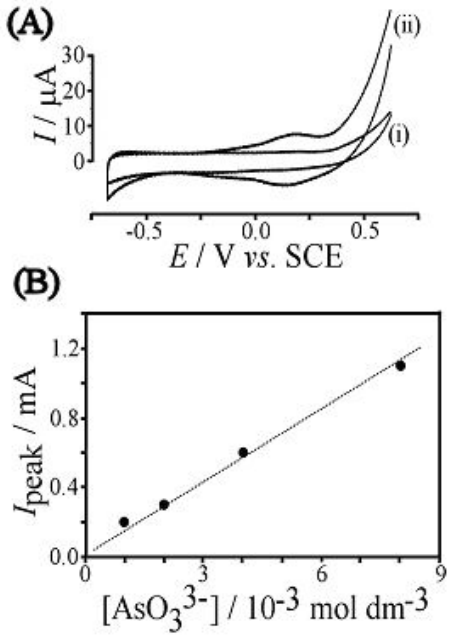

Figure 13. (A) Cyclic voltammograms (scan rate 0.1 Vs^{-1}, area 1 cm^2) for (i) a 1-layer PS-Ru^{3+} film deposit and (ii) a 15-layer PS-Ru^{3+} film deposit on ITO immersed in 1mM AsO_3^{-3} in 0.1 M phosphate buffer pH 5. (B) Plot of peak current for the AsO_3^{3-} oxidation versus the concentration of AsO_3^{-3} in 0.1 M phosphate buffer pH 5.

From this study, a novel electrocatalytic process for the arsenite (III) oxidation on PSS-Ru^{3+} was observed and it indicated that PSS-Ru^{3+} could be a useful tool in electroanalysis. Annealing or heat treatment of PSS-Ru^{3+} film was applied to stabilize the film toward dissolution and the sensivity toward arsenite is clearly improved.

In conclusion, a porous silicate from octa-anionic cage like polysilicate and Ru^{3+} cations in an ethanol based layer by layer assembly process was prepared. Electrochemical experiments confirm the formation of redox active ruthenium centers in the form of hydrous ruthenium oxide throughout the film deposition. The reduction of cationic methylene blue was shown to occur and electrocatalytic behavior of this film for oxidation of hydroquinone and arsenite was investigated. Then, potential application of this film for arsenic measurement was suggested.

4. Conclusion

This study demonstrated the use of nanomaterials particularly conductive nanomaterials including carbon nanofibers, carbon nanoparticles, and gold nanoparticles and nanoporous materials including polyhedral Silsesquioxanes, for preparation of thin film electrodes for electroanalytical purposes. It also contributed to give a better understanding of the behavior of these nanomaterials when combined with other additives in different thin films. In order to explore novel properties and understand the potential applications of these nanomaterials, different methods were applied for the fabrication of nanostructured arrays with specified geometry and surface characteristics. In this regard, the following outcome could be drawn based on this study:

- A novel type of electrode was fabricated by embedding carbon nanofibers in a thermoplastic polystyrene matrix. The 33 wt% carbon nanofiber in polystyrene was chosen as the optimum and most producible composition. Compared to conventional 3 mm glassy carbon electrode, lower capacitance current and high faradaic current was achieved for this electrode. The electrode were tested for anodic stripping voltammetry measurement of Pb^{2+} in aqueous media and modified with 1,1́-ferrocenedicarboxylic acid as internal redox reagent.
- A layer by layer film and a solvent evaporated film were prepared separately from chitosan and tosylated carbon nanoparticles on ITO/glass and glassy carbon electrode, respectively. In both film, the chitosan binder has dual effects. It effectively binds carbon nanoparticles to fabricate nanostructures and its ammonium/amine functionalities provide binding sites for physisorption and chemisorption. The chemisorbed redox system is more stable even for a wide pH range. It was shown that the convenient control of the binding site density via deposition condition provides a versatile route into for enantioselective drug sensors, or surface functionalized sensor electrodes.
- An electro-aggregated gold nanoparticle deposit on boron doped diamond electrode was characterized. The electrode was successfully applied for determination of arsenic (III) in the presence of phosphate in neutral media (phosphate buffer solution at pH 7) with low detection limit consistent with WHO requirement.
- An octa-anionic silicate cage incorporated ruthenium (III) was used to form thin film silicate structure on ITO/glass via layer by layer assembly method. This highly disordered and porous film is formed with anionic binding sites for methylene blue adsorption and electrocatalytic reactivity toward hydroquinone. The dependency of arsenite (III) electrooxidation to the arsenic(III) concentration suggested the possible application of this electrode for future arsenic electrosensors.

In brief, it can be concluded when nanoparticles are supported on an electrode surface, they can catalyze a heterogeneous electron transfer and this characteristic makes them suitable for electroanalysis and detection of species in solution. Nanoparticle-modified electrodes can display a high sensitivity due to the high surface area and the corresponding high rate of mass transport and high current density compare to bulk materials. When the surfaces of these materials are functionalized, they provide adsorption and reactive surface sites which can be used for immobilization of the opposite charged materials for designing new electrosensors.

5. References

Ajayan P.M. (1999): Nanotubes from Carbon. Chem. Rev. 99: 1787-1800.

Amiri M., Shahrokhian S., Marken F. (2007): Ultrathin Carbon Nanoparticle Composite Film Electrodes: Distinguishing Dopamine and Ascorbate. Electroanalysis 19: 1032– 1038.

Amiri M., Shahrokhian S., Psillakis E., Marken F. (2007): Electrostatic accumulation and determination of triclosan in ultrathin carbon nanoparticle composite film electrodes. Analytica Chimica Acta 593: 117-122.

Andersen J. E. T., Zhang J. -D., Chi Q., Hansen A. G., Nielsen J. U., Friis E. P., Ulstrup J. (1999): In situ scanning probe microscopy and new perspectives in analytical chemistry. Trends in Analytical Chemistry 18: 665-674.

Armelao L, Barreca D, Moraru B (2003): A molecular approach to RuO_2-based thin films: sol–gel synthesis and characterisation. J. Non-Cryst Solids 316: 364-371.

Arvinte A., Valentini F., Radoi A., Arduini R., Tamburri E., Rotariu L., Palleschi G., Bala C. (2007): The NADH electrochemical detection performed at carbonnanofibers modified glassy carbon electrode. Electroanalysis 19: 1455-1459.

Ashley K. (2003): Developments in electrochemical sensors for occupational and environmental health applications. J. Hazardous Materials 102: 1-12.

Baker. S. E., Colavita P. E., Tse K.-Y., Hamers R. J. (2006): Functionalized Vertically Aligned Carbon Nanofibers as Scaffolds for Immobilization and Electrochemical Detection of Redox-Active Proteins. J. Chem. Mater. 18: 4415-4422.

Banks C. E., Compton R. G. (2005): Edge Plane Pyrolytic Graphite Electrodes in Electronalysis: An Overview. Analytical Science 21: 1263-1268.

Bard A.J., Faulkner L.R. (2001): Electrochemical Methods-Fundamentals and Applications, 2nd. John Wiley & Sons, New York.

Bavykin D. V., Lapkin A. A., Plucinski P. K., Friedrich J. M., Walsh F. C. (2005): TiO_2 nanotube-supported ruthenium(III) hydrated oxide: A highly active catalyst for selective oxidation of alcohols by oxygen J. Catal. 235: 10-17.

Bharathi S., Fishelson N., Lev O. (1999): Direct Synthesis and Characterization of Gold and Other Noble Metal Nanodispersions in Sol-Gel-Derived Organically Modified Silicates. Langmuir 15: 1929- 1937.

Bharathi S., Nogami M., Lev O. (2001): Layer by Layer Self-Assembly of Thin Films of Metal Hexacyanoferrate Multilayers. Langmuir 17: 7468-7471.

Bharathi S., Nogami M. (2001): A glucose biosensor based on electrodeposited biocomposites of gold nanoparticles and glucose oxidase enzyme. Analyst 11: 1919-1922.

Binnig G., Rohrer H. (1985): Scanning tunneling microscope. Surface Science 152-153: 17-26.

Bobet J.-L., Grigorova E., Khrussanova M., Khristov M., Peshev P. Hydrogen sorption properties of the nanocomposite 90 wt% Mg_2Ni+10 wt% V. J. alloys and compounds 356-57: 593-597.

Bowman M.J., Booth A.D. (1997): A Review of Methods for the Examination of Magnetic Domain Structure. Materials Characterization 39: 139-167.

Brett C. M. A. (1999): Electroanalytical Techniques for the Future: The Challenges of Miniaturization and of Real-Time Measurements. Electroanalysis 11: 1013 – 1016.

Cai H., Wang Y., He P., Fang Y. (2002): Electrochemical detection of DNA hybridization based on silver-enhanced gold nanoparticle label. Analytica Chimica Acta 469: 165-172.

Cao G. (2004): Nanostructures and nanomaterials: synthesis, properties and applications. Imperial College Press, London.

Cao L., Scheiba F., Roth C., Schweiger F., Cremers C., Stimming U., Fuess H., Chen L. Q., Zhu W. T., Qiu X. P. (2006): Novel Nanocomposite Pt/RuO_2.x H2O/Carbon Nanotube Catalysts for Direct Methanol Fuel Cells. Angew Chem. 118: 5441-5445.

Céspedes F., Martinez-Fàbregas E., Alegret S. (1996): New materials for electrochemical sensing I. Rigid conducting composites. Trends in analytical Chemistry 15: 296-304.

Chen J., Tang J., Yan F., Ju H. (2006): A gold nanoparticles/sol-gel composite architecture for encapsulation of immunoconjugate for reagentless electrochemical immunoassay. Biomaterials 27: 2313-2321.

Claesson P.M., Ederth T., Bergeron V., Rutland M.W. (1996): Techniques for measuring surface forces. Advances in colloid and interface science 67: 119-183.

Collins P. G.Zettl A., Bando H., Thess A., Smalley R.E. (1997): Nanotube nanodevice. Science 278: 100-103.

Crespilho F. N., Zucolotto V., Oliveira O. N., Nart F.C. (2006): Electrochemistry of layer by layer films: a review. J. Electroch. Sci. 1: 194-214.

Crumbliss A. L., O'Daly J.P., Perine S. C., Stonehuerner J., Tubergen K.R., Zhao J., Henkens R.W. (1992): Colloidal gold as a biocompatible immobilization matrix suitable for the fabrication of enzyme electrodes by electrodeposition. Biotechnol. Bioeng. 40: 483-490.

Dai H., Hafner J. H., Rinzler A. G., Colbert D. T., Smalley R. E. (1996): Nanotubes as nanoprobes in scanning probe microscopy. Nature 384: 147 – 150.

Dai, X.; Nekrassova, O.; Hyde, M. E.; Compton, R. G. (2004): Anodic stripping voltammetry of arsenic (III) using gold nanoparticle-modified electrodes. Anal. Chem. 76: 5924-5929.

Dai X., Compton R. G. (2005): Gold nanoparticle modified electrodes show a reduced interference by Cu (II) in the detection of As (III) using anodic stripping voltammetry. Electroanalysis 17: 1325-1330.

Dai X., Nekrassova O., Hyde M. E., Compton R. G. (2004): Anodic stripping voltammetry of arsenic (III) using gold nanoparticle-modified electrodes. Anal. Chem. 76: 5924-5929.

Dalmas F., Chazeaul L., Gauthuthier C., Masenelli-Varlotk K., Dendievel R., Cavaille J. Y., Forro L. (2005): Multiwalled carbon nanotube/polymer nanocomposites : Processing and properties. J. Polymer science. Part B. Polymer physics 43: 1186-1197.

Daniel M. C., Astruc D. (2004): Gold Nanoparticles: Assembly, Supramolecular Chemistry, Quantum-Size-Related Properties, and Applications toward. Chem. Rev. 104: 293-346.

Decher (1997): Fuzzy nanoassemblies. Science 277 (5330): 1232-1237.

Dijk N. V., Fletcher S., Madden C. E., Marken F. (2001): Nanocomposite electrodes made of carbon nanofibers and black wax. Anodic stripping voltammetry of zinc and lead. Analyst 126: 1878-1881.

Dutta P.K., Vaidyalingam A. S. (2003): Zeolite-supported ruthenium oxide catalysts for photochemical reduction of water to hydrogen. Microporous and Mesoporous Materials 62: 107-120.

Fachinotti E., Guerrini E., Tavares A. C., Trasatti S. (2007): Electrocatalysis of H_2 evolution by thermally prepared ruthenium oxide: Effect of precursors: Nitrate vs. chloride J. Electroanal. Chem. 600: 103-112.

Fisher A. C. (1996): Electrode dynamic. Oxford University press Inc. New York.

Forsberg G., O'Laughlin J.W., Megargle R.G., Koirtyihann S.R. (1975): Determination of arsenic by anodic stripping voltammetry and differential pulse anodic stripping voltammetry. Anal. Chem. 47: 1586-1592.

Fukuda T., Arai F., Lixin D., Imaizumi Y. (2004): Perspective of nanotube sensors and nanotube actuators. 4th IEEE Conference on Nanotechnology. 41 – 44.

Gajic -Krstaji L. M., Trisovic T. Lj., Krstaji N. V. (2004): Spectrophotometric study of the anodic corrosion of Ti/RuO_2 electrode in acid sulfate solution. Corrosion Science 46: 65-74.

Hao, C.,Ding, L.,Hang, X.,Ju, H. (2007): Biocompatible Conductive Architecture of Carbon Nanofiber-Doped Chitosan Prepared with Controllable Electrodeposition for Cytosensing. Anal. Chem. 79: 4442-4447.

Hayashi A., Yamamoto S., Suzuki K., Matsuoka T. (2004): The first application of fullerene polymer-like materials, $C_{60}Pd_n$, as gas adsorbents. J. Mater. Chem. 14: 2633-2637.

Heath J. R. (1995): The Chemistry of Size and Order on a Nanometer Scale. Science 270: 1315-1316.

Horisberger M. (1981): Colloidal gold: a cytochemical marker for light and fluorescent microscopy and for transmission and scanning electron microscopy. Scanning electron micros. 2: 9- 31.

Iijima S. (1991): Helical microtubules of graphitic carbon. Nature 354: 56-58.

Idegami K., Chikae M., Kerman K., Nagatani N., Yuhi T., Endo T., Tamiya E. (2007): Gold nanoparticle-based redox signal enhancement for sensitive detection of human chorionic Goandrotropin Hormone. Electroanalysis 20: 14-21.

Jirkovsky J, Makarova M, Krtil P (2006): Particle size dependence of oxygen evolution reaction on nanocrystalline RuO_2 and $Ru_{0.8}Co_{0.2}O_{2-x}$. Electrochem Commun 8: 1417-1422.

Katz E., Willner I., Wang J. (2004): Electroanalytical and bioelectroanalytical systems based on metal and semiconductor nanoparticles. Electroanalysis 16: 19-44.

Kojima Y., Usuki A., Kawasumi M., Okada A., Kurauchi T., and Kamigaito O. (1993): Synthesis of nylon 6-clay hybrid by montmorillonite intercalated with ε-caprolactam. J. Polymer Science Part A: Polymer Chemistry 31: 983-986.

Kresge C. T., Leonowicz M. E., Roth W. J., Vartuli J. C., Beck J. S. (1992): Ordered mesoporous molecular sieves synthesized by a liquid-crystal template mechanism. Nature 359: 710 – 712.

Kroto H. W., Heath J. R., O'Brien S. C., Curl R. F., Smalley R. E. (1985): C60: Buckminsterfullerene. Nature 318: 162–163.

Kuroki M, Asefa T, Whitnal W, Kruk M, Yoshina-Ishii C, Jaroniec M, Ozin GA (2002): Synthesis and Properties of 1,3,5-Benzene Periodic Mesoporous Organosilica (PMO): Novel Aromatic PMO with Three Point Attachments and Unique Thermal Transformations. J. Am. Chem. Soc. 124: 13886-13895.

Lin H. B., Shih J.S. (2003): Fullerene C60-cryptand coated surface acoustic wave quartz crystal sensor for organic vapors. Sensors and Actuators B: Chemical 92: 243-254.

Liu T., Tang J., Han M., Jiang L. (2003): A novel microgravimetric DNA sensor with high sensitivity. Biochemical and Biophysical Research Communications 304: 98-100.

Liu T., Tang J., Han M., Jiang L. (2004): The enhancement effect of gold nanoparticles as a surface modifier on DNA sensor sensitivity. Biochemical and Biophysical Research Communications 313: 3-7.

Liu, G., Lin, Y.-Y., Wu, H., Lin, Y. (2007): Voltammetric Detection of Cr(VI) with Disposable Screen-Printed Electrode Modified with Gold Nanoparticles. Environmental science & Technology 41: 8129-8134.

Lu L. P., Wang S. Q., Lin X. Q. (2004): Fabrication of layer-by-layer deposited multilayer films containing DNA and gold nanoparticle for norepinephrine biosensor. Analytica chimica acta 519: 161-166.

MacDonald S. M., Fletcher P.D.I., Cui Z. G., Opallo M., Chen J., Marken F. (2007): Carbon nanoparticle stabilised liquidliquid micro-interfaces for electrochemically driven ion-transfer processes. Electrochimica Acta 53: 1175-1181.

MacDonald S. M., Szot K., Niedziolka J., Marken F., Opallo M. (2008): Introducing hydrophilic carbon nanoparticles into hydrophilic sol-gel film electrodes. J. Solid State Electrochemistry 12: 287-293.

Marchesan S., Ros T.D., Spalluto G., Balzarini J., Prato M. (2005): Anti-HIV properties of cationic fullerene derivatives. Bioorganic & Medicinal Chemistry Letters 15: 3615-3618.

Margadonna S., Prassides K. (2002): Recent Advances in Fullerene Superconductivity. J. of Solid State Chemistry 168: 639-652.

Marken F., Gerrard M. L., Mellor I. M., Mortimer R.J., Madden C.E, Fletcher S., Holt K. Foord J.S., Dahm R.H., Page F. (2001): Voltammetry at carbon nanofiber electrodes. Electrochemistry Communications 3: 177-180.

Maruyama S. http://www.photon.t.u-tokyo.ac.jp/~maruyama/ , last access 11.06.2008

Mazurek M, Benker N, Roth C, Fuess H (2006): Binary Mixtures of Carbon Supported Pt and Ru Catalysts for PEM Fuel Cells. Fuel Cells 6: 208-214.

Merkoçi A. (2007): Nanobiomaterials in electroanalysis. Electroanalysis 19: 739-741.

Mirkin C.A., Caldwell W.B. (1996): Thin film, fullerene-based materials. Tetrahedron 52: 5113-5130.

Miyata N., Yamakoshi Y. (1999): Fullerene: a photosensitizer effectively generates oxyl radicals to cause DNA cleavage. Free Radical Biology and Medicine 27: S96.

Murphy M. M., Wilcox G.D., Dahm R.H., Marken F. (2003): Adsorption and redox processes at carbon nanofiber electrodes grown onto a ceramic fiber backbone. Electrochemistry communications 5: 51-55.

Musameh M., Wang J., Merkoci A., Lin Y. (2002): Low-potential stable NADH detection at carbon-nanotube-modified glassy carbon electrodes. Electrochemistry Communications 4: 743-746.

Niedziolka J., Murphy M. A., Marken F., Opallo M. (2006): Characterization of hydrophobic carbon nanofiber–silica composite film electrodes for redox liquid immobilization. Electrochimica Acta 51: 5897-5903.

Ozine G.A. (1992): Nanochemistry: Synthesis in diminishing dimensions. Adv. Mater. 4: 612-649.

Pan M., Guo X., Cai Q., Li G., Chen Y. (2003): A novel glucose sensor system with Au nanoparticles based on microdialysis and coenzymes for continuous glucose monitoring. Sensors and Actuators A: Physical 108: 258-262.

Penn S. G., He L., Natan M. J. (2003): Nanoparticles for bioanalysis. Current opinion in chemical biology 7: 609-615.

Pimtong-Ngam Y., Jiemsirilers S., Supothina S. (2006): Preparation of tungsten oxide–tin oxide nanocomposites and their ethylene sensing characteristics. Sensors and Actuators A: Physical 139:7-11.

Price R. L., Waid M. C., Haberstroh K. M., Webster T. J. (2003): Selective bone cell adhesion on formulations containing carbon nanofibers. Biomaterials 24: 1877-1887.

Pruneanu S., Ali Z., Watson G., Hu S. Q., Lupu D., Biris A.R., Olenic L., Mihailescu G. (2006): Investigation of electrochemical properties of carbon nanofibers prepared by CCVD method. Particulate science and technology 24: 311-320.

Pumera M., Sánchez S., Ichinose I., Tang J. (2007): Electrochemical nanobiosensors. Sensors and ActuatorsB.123:1195-1205.

Raj C. R., Okajima T., Ohsaka T. (2003): Gold nanoparticle arrays for the voltammetric sensing of dopamine. J. Electroanalytical Chemistry 543: 127-133.

Randles J. E. B. (1948): A cathode ray polarograph. Part II. — The current-voltage curves. Trans. Faraday Soc. 44: 327-337.

Ren Z. F., Huang Z. P., Xu J.W., Wang J.H.,Bush P., Seigal M. P., Provencio P. N. (1998): Synthesis of large arrays of well-alligned carbon nanotubes on glass. Science 282: 1105-1107.

Rosi N. L., Mirkin C. (2005): Nanostructures in biodiagnostics. Chem. Rev. 105: 1547-1562.

Rozniecka E., Niedziolka J., Murphy M.A., Sirieix-Plenet J., Gaillon L., Marken F., Opallo M. (2006): Ion transfer processes at the room temperature ionic liquidaqueous solution interface supported by a hydrophobic carbon nanofibers – silica composite film. J. Electroanal. Chem. 587: 133-139.

Safavi A., Maleki N., Moradlou O., Tajabadi F. (2006): Simultaneous determination of dopamine, ascorbic acid, and uric acid using carbon ionic liquid electrode. Analytical Biochemistry 359: 224-229.

Scholz. F. (editor) (2002): Electroanalytical methods: Guide to experiments and applications. Springer publications.

Schüth F., Schmidt W. (2002): Microporous and mesoporous materials. Advanced Engineering Materials 4: 269 – 279.

Sherrington I., Smith E. H. (1988): Modern measurement techniques in surface metrology: part I; stylus instruments, electron microscopy and non-optical comparators. Wear 125: 271-288.

Shih J.S., Chao Y. C., Sung M.F., Gau G. J., Chiou C. (2001): Piezoelectric crystal membrane chemical sensors based on fullerene C60. Sensors and Actuators B: Chemical 76: 347-353.

Shiraishi H., Itoh T., Hayashi H., Takagi K., Sakane M., Mori T., Wang J. (2007): Electrochemical detection of E. coli 16S rDNA sequence using air-plasma-activated fullerene-impregnated screen printed electrodes. Bioelectrochemistry 70: 481-487.

Shokouhimehr M., Piao Y., Kim J., Jang Y., Hyeon T. (2007): A Magnetically Recyclable Nanocomposite Catalyst for Olefin Epoxidation. Angewandte Chemie 119: 7169 – 7173.

Shul G., Murphy M. M., Wilcox G. D., Marken F., Opallo M. (2005): Effects of carbon nanofiber composites on electrode processes involving liquid|liquid ion transfer. J. Solid State Electrochemistry 9: 874-881.

Singha, S., Thomas, M.J. (2006): Polymer composite/nanocomposite processing and its effect on the electrical properties. IEEE Conference on Electrical Insulation and Dielectric Phenomena 557 – 560.

Song M-K., Park S-B., Kim Y-B, Kim K-H, Min S-K, Rhee H-W. (2004): Characterization of polymer-layered silicate nanocomposite membranes for direct methanol fuel cells. Electrochimica Acta 50: 639-643.

Steigerwalt, E. S., Deluga, G. A., Lukehart, C. M. (2002): Pt-Ru/Carbon Fiber Nanocomposites: Synthesis, Characterization, and Performance as Anode Catalysts of Direct Methanol Fuel Cells. A Search for Exceptional Performance. J. Phys. Chem. B. 106: 760-766.

Stott S. J., Mortimer R. J., Dann S. E., Oyama M., Marken F. (2006): Electrochemical properties of core-shell TiC–TiO_2 nanoparticle films immobilized at ITO electrode surfaces**.** Phys. Chem. Chem. Phys. 46: 5437-5443.

Su L., Mao L.Q. (2006): Gold nanoparticle/alkanedithiol conductive films self-assembled onto gold electrode: Electrochemistry and electroanalytical application for voltammetric determination of trace amount of catechol. Talanta 70: 68-74.

Tang D.P., Yuan R., Chai Y.Q., Zhong X. , Liu Y., Dai J.Y. , Zhang L.Y. (2004): Novel potentiometric immunosensor for hepatitis B surface antigen using a gold nanoparticle-based biomolecular immobilization method.Analytical biochemistry 333: 345-350.

Treacy M. M. J., Ebbesen T.W., Gilbson J.M. (1996): Exceptionally high Young's modulus observed for individual carbon nanotubes. Nature 381: 678-680.

Vamvakaki, V., Tsagaraki, K.,Chaniotakis, N. (2006): Carbon Nanofiber-Based Glucose Biosensor. Anal. Chem. 78: 5538-5542.

Vansteenkiste S. O., Davies M. C., Roberts C. J., Tendler S.J.B., Williams P.M. (1998): Scanning probe microscopy of biomedical interfaces. Progress in Surface Science 57: 95-136.

Vieira R., Pham-Huu C., Keller N., Ledoux M.J. (2003): Carbon nanofibers a new catalyst support for hydrazine decomposition. Quimica Nova 26: 665-669.

Wang J. (2000): Analytical electrochemistry. Second edition Wiley-VCH.

Wang J. (2005): Nanomaterial-based electrochemical biosensors. Analyst 130: 421-426.

Wang L., Bai J., Huang P., Wang H., Zhang L., Zhao Y. (2006): Self-assembly of gold nanoparticles for the voltammetric sensing of epinephrine. Electrochemistry communication 8: 1035-1040.

Welch C. M., Nekrassova O., Dai X., Hyde M. E., Compton R. G. (2004): Fabrication, characterization and voltammetric studies of gold amalgam nanoparticle modified electrodes. Chem Phys Chem. 5: 1405-1410.

Welch C.M., Compton R.G. (2006): The use of nanoparticles in electroanalysis: a review. Anal. Bioanal. Chem. 384: 601-619.

Wu L., McIntosh M., Zhang X., Ju (2007): Amperometric sensor for ethanol based on one-step electropolymerization of thionine–carbon nanofiber nanocomposite containing alcohol oxidase. Talanta 74: 387-392.

Wu L., Yan F., Ju H. (2007): An amperometric immunosensor for separation-free immunoassay of CA125 based on its covalent immobilization coupled with thionine on carbon nanofibers. J. Immunological Methods 322: 12-19.

Wu, L.; Zhang, X.; Ju, H. (2007): Detection of NADH and Ethanol Based on Catalytic Activity of Soluble Carbon Nanofiber with Low Overpotential. Anal. Chem. 79: 453-458.

Wu L., Zhang X., Ju H. (2007): Amperometric glucose sensor based on catalytic reduction of dissolved oxygen at soluble carbon nanofibers. Biosensors and Bioelectronics 23: 479-484.

Yoon S. H., Lim S., Song Y., Ota Y., Qiao W., Tanaka A., Mochida I. (2004): KOH activation of carbon nanofibers. Carbon 42: 1723-1729.

Yáňez-Sedeňo P., Pingarrón J. M. (2005): Gold nanoparticle-based electrochemical biosensors. Anal. Bioanal. Chem. 382: 884-886.

Zhang B., Yao N., Wang X., Ma H., Zhang L., Wang S., Wei J. (2001): A flat panel display device fabricated by using carbon nanotubescathode. Microelectronics Conference IVMC Proceedings of the 14th International 193 – 194.

Zhang J., Oyama M. (2004): A hydrogen peroxide sensor based on the peroxidase activity of hemoglobin immobilized on gold nanoparticles-modified ITO electrode. Electrochimica Acta 50: 85-90.

Zhang Z. L., Pang D. W., Yuan H., Cai R. X., Abruña H. D. (2005): Electrochemical DNA sensing based on gold nanoparticle amplification. Analytical and Bioanalytical Chemistry 381: 833-838.

Zhou Z., Yang J., Zhang Y., Chang L., Sun W., Wang J. (2006): NaA zeolite/carbon nanocomposite thin films with high permeance for CO_2/N_2 separation. Separation and Purification Technology 55: 392-395.

Zimer A. M., Bertholdo R., Grassi M.T., Zarbin A.J.G., Mascaro L.H. (2003): Template carbon dispersed in polyaniline matrix electrodes: evaluation and application as electrochemical sensors to low concentrations of Cu^{2+} and Pb^{2+}. Electrochemistry Communications.5:938-988.

Kuopio University Publications C. Natural and Environmental Sciences

C 213. Georgiadis, Stefanos. State-Space Modeling and Bayesian Methods for Evoked Potential Estimation.
2007. 179 p. Acad. Diss.

C 214. Sierpowska, Joanna. Electrical and dielectric characterization of trabecular bone quality.
2007. 92 p. Acad. Diss.

C 215. Koivunen, Jari. Effects of conventional treatment, tertiary treatment and disinfection processes on hygienic and physico-chemical quality of municipal wastewaters.
2007. 80 p. Acad. Diss.

C 216. Lammentausta, Eveliina. Structural and mechanical characterization of articular cartilage and trabecular bone with quantitative NMR .
2007. 89 p. Acad. Diss.

C 217. Veijalainen, Anna-Maria. Sustainable organic waste management in tree-seedling production.
2007. 114 p. Acad. Diss.

C 218. Madetoja, Elina. Novel process line approach for model-based optimization in papermaking.
2007. 125 p. Acad. Diss.

C 219. Hyttinen, Marko. Formation of organic compounds and subsequent emissions from ventilation filters.
2007. 80 p. Acad. Diss.

C 220. Plumed-Ferrer, Carmen. Lactobacillus plantarum: from application to protein expression.
2007. 60 p. Acad. Diss.

C 221. Saavalainen, Katri. Evaluation of the mechanisms of gene regulation on the chromatin level at the example of human hyaluronan synthase 2 and cyclin C genes.
2007. 102 p. Acad. Diss.

C 222. Koponen, Hannu T. Production of nitrous oxide (N_2O) and nitric oxide (NO) in boreal agricultural soils at low temperature.
2007. 102 p. Acad. Diss.

C 223. Korkea-aho, Tiina. Epidermal papillomatosis in roach (Rutilus rutilus) as an indicator of environmental stressors.
2007. 53 p. Acad. Diss.

C 224. Räisänen, Jouni. Fourier transform infrared (FTIR) spectroscopy for monitoring of solvent emission rates from industrial processes.
2007. 75 p. Acad. Diss.

C 225. Nissinen, Anne. Towards ecological control of carrot psyllid (Trioza apicalis).
2008. 128 p. Acad. Diss.

C 226. Huttunen, Janne. Approximation and modellingerrors in nonstationary inverse problems.
2008. 56 p. Acad. Diss.

C 227. Freiwald, Vera. Does elevated ozone predispose northern deciduous tree species to abiotic and biotic stresses?
2008. 109 p. Acad. Diss.